LUND UNIVERSITY

The direct and inverse problem for obliquely incident transient elastodynamic waves

Hellberg, Rasmus; Karlsson, Anders

1997

Link to publication

Citation for published version (APA):
Hellberg, R., & Karlsson, A. (1997). *The direct and inverse problem for obliquely incident transient elastodynamic waves*. (Technical Report LUTEDX/(TEAT-7057)/1-27/(1997); Vol. TEAT-7057). [Publisher information missing].

Total number of authors:
2

General rights
Unless other specific re-use rights are stated the following general rights apply:
Copyright and moral rights for the publications made accessible in the public portal are retained by the authors and/or other copyright owners and it is a condition of accessing publications that users recognise and abide by the legal requirements associated with these rights.
• Users may download and print one copy of any publication from the public portal for the purpose of private study or research.
• You may not further distribute the material or use it for any profit-making activity or commercial gain
• You may freely distribute the URL identifying the publication in the public portal

Read more about Creative commons licenses: https://creativecommons.org/licenses/

Take down policy
If you believe that this document breaches copyright please contact us providing details, and we will remove access to the work immediately and investigate your claim.

LUND UNIVERSITY

PO Box 117
221 00 Lund
+46 46-222 00 00

Download date: 09. Jun. 2026

CODEN:LUTEDX/(TEAT-7057)/1-27/(1997)

The direct and inverse problem for obliquely incident transient elastodynamic waves

Rasmus Hellberg and Anders Karlsson

Department of Electroscience
Electromagnetic Theory
Lund Institute of Technology
Sweden

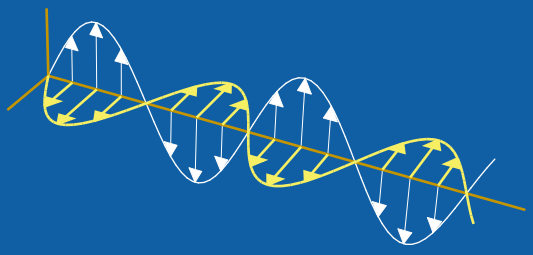

Rasmus Hellberg

Department of Electromagnetic Theory
Royal Institute of Technology
S-100 44 Stockholm
Sweden

Anders Karlsson

Department of Electroscience
Electromagnetic Theory
Lund Institute of Technology
P.O. Box 118
SE-221 00 Lund
Sweden

Editor: Gerhard Kristensson
© Rasmus Hellberg and Anders Karlsson, Lund, May 21, 1997

Abstract

The direct and inverse scattering problems for a plane-stratified viscoelastic medium excited by a transient plane wave of SH or P-SV type are treated. The viscoelastic medium is characterized by two time and space dependent memory functions and a spatially dependent density. The direct and inverse problems are solved by a time-domain wave propagator method that is related to the Green functions technique and the imbedding method. The definition of the wave-propagators is based upon a wave-splitting technique where the total wave is split into generalized left and right going components. A numerical algorithm for the inverse problem is presented for the P-SV case.

1 Introduction

In this paper, the direct and inverse scattering for inhomogeneous viscoelastic media are treated in the time-domain. The inverse problems are important in several areas of elastodynamics, e.g. in non-destructive media evaluation, in seismology, and in the design of media with prescribed reflection and transmission properties. Viscoelastic media are characterized by a constitutive relation which is non-local in time. In this relation stress and displacement are related to each other by memory functions. A consequence of the non-local time dependence is that viscoelastic media are dissipative as well as dispersive.

Viscoelastic media support both shear (S) waves and pressure (P) waves. Here, the viscoelastic medium is one-dimensional and is excited by a transient incident plane wave. The shear wave is decomposed in two polarizations, the horizontal shear wave (SH wave) and the vertical shear wave (SV wave). The pressure wave has only one state of polarization. At oblique incidence, the SH wave is uncoupled to the other two modes, whereas the SV and P waves couple. Both of these two cases, the SH and the P-SV case, are analyzed in this paper. The direct and inverse problems are treated by a time-domain wave propagator method. The method is based upon a wave splitting technique where the waves are decomposed in generalized left and right moving waves. Two closely related methods are the imbedding method and the Green functions approach. The relations between these three methods are discussed in the paper. In all three methods scattering operators that map the split fields at one position to the split fields at another position are introduced. A significant feature is that the operators are independent of the incident field.

Most of the development of the imbedding method, the Green functions approach and the propagator method has taken place in the area of electromagnetics, cf. [13, 15–18, 20, 21, 23–26]. However, in the early history of these methods, there were some papers that dealt with the elastodynamic and acoustic cases, and these papers are related to the present paper. Thus in [2], [19] and [9] the viscoelastic SH case was analyzed by the imbedding method and in [11] the P-SV case was analyzed by the imbedding method. Recently, a number of new and interesting results concerning transient direct and inverse scattering for the Timoshenko beam equation have been reported [3, 4, 12, 27]. The imbedding method and the Green functions approach were used in these papers. The wave splitting for the Timoshenko beam equation

is more complicated than the one for a viscoelastic medium but otherwise there are both analytical and numerical similarities between the two cases. All of the above references concern one-dimensional wave propagation, but there are promising results for the imbedding and Green functions approach for the three dimensional case, see [30].

The current time domain wave propagator method has similarities with the frequency domain method referred to as the propagator matrix method. This method has been successfully used for several years in elastodynamics, see [22] and earlier references. The propagator matrix method is not based upon the concept of wave splitting, and it is far from being the frequency domain counterpart of the time domain method presented in this paper. There are a vast number of papers in books and journal articles on other frequency domain methods for wave propagation in elastic and viscoelastic media. For the SH case and the uncoupled P-SV case, i.e. for normal incidence or homogeneous media, a common method for the inverse problem is to transform the equations to the Schrödinger equation and use methods developed for the inverse potential problem, see e.g. [29]. Other examples of frequency domain methods for the one-dimensional inverse P-SV problem are [7] and [6]. A number of time domain methods for the inverse problem have also been developed. A review of methods related to the method of characteristics is found in [5]. Most methods for the inverse problem rely on reflection data, but there are also methods that use transmission data for reconstructions, cf [14].

The outline of the paper is as follows: The constitutive relation and the basic quantities are introduced in Section 2. In Section 3, the wave equation is derived and the wave splitting technique is applied. The wave propagators are introduced in Section 4, and in Section 5 the relation between the propagator method, the imbedding method and the Green functions approach is discussed. The propagators are operators that can be represented in terms of propagator integral kernels. Two different sets of equations for these kernels are derived in Section 6. The direct and inverse problems are defined and discussed in Section 7, where a numerical algorithm for the inverse problem is presented, too. Finally, one numerical example is presented in Section 8. The example concerns simultaneous reconstruction of three independent functions: the density and the spatial dependence of the two memory functions.

2 Formulation of the problem

The time domain constitutive relation for an isotropic viscoelastic medium relates the stress tensor $\boldsymbol{\Sigma}(x, y, z, t')$ to the displacement vector $\boldsymbol{u}$

$$\boldsymbol{\Sigma} = \boldsymbol{I}\,\partial_{t'}\left[E * \nabla\cdot\boldsymbol{u}\right] + 2\partial_{t'}\left[G * (\nabla\boldsymbol{u} - \boldsymbol{I}\,\nabla\cdot\boldsymbol{u})\right] + \partial_{t'}\left[G * \boldsymbol{I}\times(\nabla\times\boldsymbol{u})\right], \qquad (2.1)$$

where the displacement vector reads

$$\boldsymbol{u}(x, y, z, t') = u(x, y, z, t')\,\hat{e}_x + v(x, y, z, t')\,\hat{e}_y + w(x, y, z, t')\,\hat{e}_z.$$

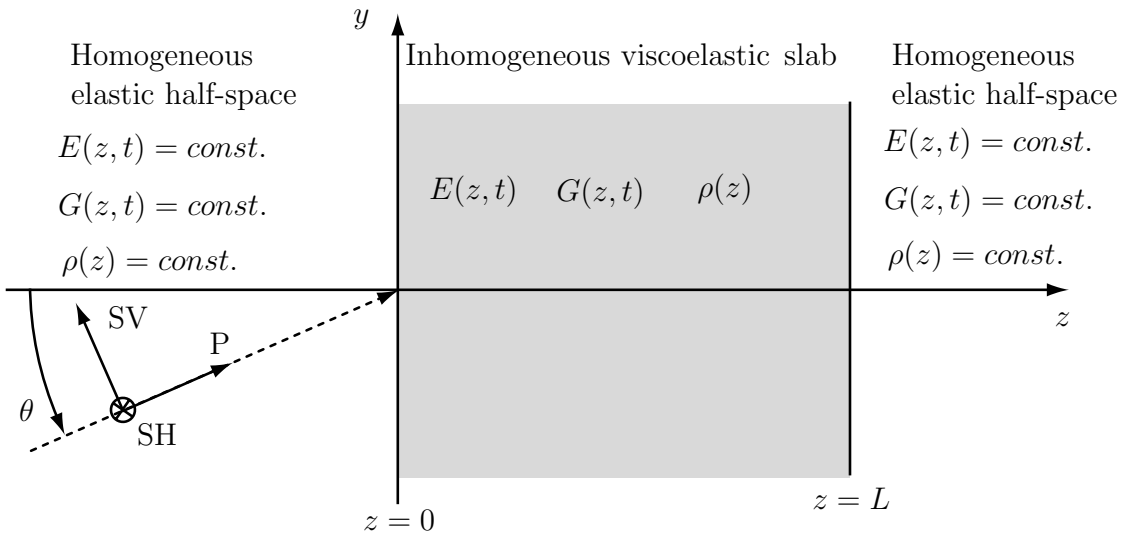

Figure 1: The geometry of the problem with the polarizations of the SH, SV and P modes.

In Eq. (2.1), $\boldsymbol{I}$ is the unit tensor and the star $*$ denotes time convolution

$$[f * g](t') = \int_0^{t'} f(t' - t'')g(t'')\, dt''.$$

The kernel $E(z, t')$ in Eq. (2.1) is the elasticity relaxation modulus and $G(z, t')$ is the shear relaxation modulus. In this time domain model, the stress due to the applied strain thus depends on the history of the strain. Examples of time domain elasticity and shear relaxation modulus can be found in e.g. [1]. In the present problem, the geometry is one-dimensional and hence $E(z, t')$ and $G(z, t')$ vary with depth z and time t'.

The wave front speed of the transverse shear waves SH and SV, and the longitudinal P wave read

$$\begin{aligned} c_{\mathrm{t}}(z) &= \sqrt{\tfrac{G(z,0)}{\rho(z)}} \\ c_{\mathrm{l}}(z) &= \sqrt{\tfrac{E(z,0)}{\rho(z)}}, \end{aligned}$$

where $\rho(z)$ is the density of the medium. Note that the longitudinal P wave travels at a higher speed than the transverse SV and SH waves, i.e. $c_{\mathrm{t}}(z) < c_{\mathrm{l}}(z)$.

The stratified viscoelastic slab occupies the region $0 \le z \le L$ and the surrounding half-spaces $z < 0$ and $z > L$ are homogeneous elastic half-spaces where $G(z, t')$ and $E(z, t')$ are constant in time and space, see Figure 1. It is assumed that the impedances for the SH, SV and P modes are continuous at the interfaces $z = 0$ and $z = L$, cf. Eq. (3.8). The incident plane wave is a transient plane wave of SV, SH or P type and the objective is to solve the direct and inverse scattering problem. In the direct problem, the material parameters and the incident field are known and the displacement vector for the reflected, transmitted and internal fields are to be determined. In the inverse problem, the incident field is known and the material parameters are to be determined from the displacement vector of the reflected field.

3 The wave equation

Consider an incident wave in the yz-plane, see Figure 1. Since the geometry of the problem is independent of y, the y coordinate can be eliminated by introducing a translated time, $t = t(t', y)$, cf. [21]. Then the derivatives with respect to y are transformed to derivatives with respect to t. The translated time is defined by

$$\begin{cases} t & = t(t', y) = t' - \alpha y \\ \alpha & = \dfrac{\sin\theta}{c_0} \\ \partial_y & = -\alpha \partial_t, \end{cases} \tag{3.1}$$

where c_0 is the wave speed of the incident wave and θ is the incident angle.

The equation of motion combined with the constitutive relation in Eq. (2.1) results in the wave equation for the displacement vector

$$\begin{aligned} \rho \partial_t^2 \boldsymbol{u} &= \nabla \cdot \boldsymbol{\Sigma} \\ &= \nabla \left(\partial_t \left[E * \nabla \cdot \boldsymbol{u} \right] \right) - \nabla \times \left(\partial_t \left[G * \nabla \times \boldsymbol{u} \right] \right) + 2 \partial_t \left[(\nabla G * \times \nabla) \times \boldsymbol{u} \right]. \end{aligned} \tag{3.2}$$

From this equation, it is seen that the wave equation can be written in terms of a scalar potential ϕ_{p} and a vector potential $\boldsymbol{\phi}_{\mathrm{s}} = (\phi_{\mathrm{s}x}, \phi_{\mathrm{s}y}, \phi_{\mathrm{s}z})$

$$\begin{cases} \boldsymbol{\phi}_{\mathrm{s}} & = \partial_t \left[G * \nabla \times \boldsymbol{u} \right] \\ \phi_{\mathrm{p}} & = \partial_t \left[E * \nabla \cdot \boldsymbol{u} \right]. \end{cases}$$

For a homogeneous medium, the scalar potential ϕ_{p} defines the pressure wave and the vector potential $\boldsymbol{\phi}_{\mathrm{s}}$ defines the shear waves. Then the x component of $\boldsymbol{\phi}_{\mathrm{s}}$ is the SV potential and the y component is the SH potential, cf. [10]. The wave equation in terms of the potentials reads

$$\rho(z) \partial_t^2 \boldsymbol{u} = \nabla \cdot \boldsymbol{\Sigma} = \begin{pmatrix} \partial_z \phi_{\mathrm{s}y} + \alpha^2 \partial_t \partial_t \left[G * \partial_t u \right](t) \\ -\alpha \partial_t \phi_{\mathrm{p}} - \partial_z \phi_{\mathrm{s}x} - 2\alpha \partial_t \left[\partial_z G * \partial_t w \right](t) \\ \partial_z \phi_{\mathrm{p}} - \alpha \partial_t \phi_{\mathrm{s}x} + 2\alpha \partial_t \left[\partial_z G * \partial_t v \right](t) \end{pmatrix}. \tag{3.3}$$

Now, introduce the following vector $\boldsymbol{\phi}$

$$\boldsymbol{\phi} = \begin{pmatrix} \phi_{\mathrm{s}y} \\ \phi_{\mathrm{s}x} \\ \phi_{\mathrm{p}} \end{pmatrix} = \begin{pmatrix} \partial_t [G * \partial_z] & 0 & 0 \\ 0 & -\partial_t [G * \partial_z] & -\alpha \partial_t [G * \partial_t] \\ 0 & -\alpha \partial_t [E * \partial_t] & \partial_t [E * \partial_z] \end{pmatrix} \begin{pmatrix} u \\ v \\ w \end{pmatrix}. \tag{3.4}$$

This relation can be inverted by introducing the resolvent kernels $h(z,t)$ and $f(z,t)$ such that

$$\partial_z \begin{pmatrix} u \\ v \\ w \end{pmatrix} = \begin{pmatrix} \frac{1}{G(z,0)} [(1 - h*) \phi_{\mathrm{s}y} \\ \frac{1}{G(z,0)} [(h * -1) \left(\phi_{\mathrm{s}x} + \alpha \partial_t [G * \partial_t w] \right) \\ \frac{1}{E(z,0)} [(1 - f*) \left(\phi_{\mathrm{p}} + \alpha \partial_t [E * \partial_t v] \right) \end{pmatrix}. \tag{3.5}$$

This equation together with Eq. (3.4) give the equations for the kernels $h(z,t)$ and $f(z,t)$

$$\begin{cases} G_t(z,t) = G(z,0)h(z,t) + [G_t(z,\cdot) * h(z,\cdot)](t) \\ E_t(z,t) = E(z,0)f(z,t) + [E_t(z,\cdot) * f(z,\cdot)](t). \end{cases} \tag{3.6}$$

Since $G(z,0) > 0$ and $E(z,0) > 0$ these equations are Volterra equations of the second kind and hence uniquely solvable.

The wave equation (3.3), can now be written in a matrix notation in terms of the displacement field $\boldsymbol{u}$ and the vector $\boldsymbol{\phi}$ utilizing Eq. (3.5)

$$\partial_z \begin{pmatrix} \boldsymbol{u} \\ \boldsymbol{\phi} \end{pmatrix} = \boldsymbol{\mathcal{A}} \begin{pmatrix} \boldsymbol{u} \\ \boldsymbol{\phi} \end{pmatrix}, \tag{3.7}$$

where the 6×6 matrix valued operator $\boldsymbol{\mathcal{A}}$ reads

$$\boldsymbol{\mathcal{A}} = \begin{pmatrix} 0 & 0 & 0 & \frac{1}{G(z,0)}[1 - h*] & 0 & 0 \\ 0 & 0 & -\alpha\partial_t & 0 & 0 & 0 \\ 0 & \alpha\partial_t & 0 & 0 & 0 & 0 \\ \rho\partial_{tt} - \alpha^2\partial_{tt}[G * \partial_t] & 0 & 0 & 0 & 0 & 0 \\ 0 & -\rho\partial_{tt} & -2\alpha\partial_t[G_z * \partial_t] & 0 & 0 & 0 \\ 0 & -2\alpha\partial_t[G_z * \partial_t] & \rho\partial_{tt} & 0 & 0 & 0 \end{pmatrix}$$
$$\begin{pmatrix} 0 & 0 \\ -\frac{1}{G(z,0)}[1 - h*] & 0 \\ 0 & \frac{1}{E(z,0)}[1 - f*] \\ 0 & 0 \\ 0 & -\alpha\partial_t \\ \alpha\partial_t & 0 \end{pmatrix}.$$

3.1 Wave splitting

A wave splitting is applied to the wave equation so that the displacement field $\boldsymbol{u}$ and the potential $\boldsymbol{\phi}$ are transformed into new independent variables, the split fields $\boldsymbol{u}^{\pm}$. The split fields form the basis for the representation of the wave propagators presented in the next section. The split fields read

$$\boldsymbol{u}^+ = \begin{pmatrix} u^+_{\mathrm{sh}} \\ u^+_{\mathrm{sv}} \\ u^+_{\mathrm{p}} \end{pmatrix}, \qquad \boldsymbol{u}^- = \begin{pmatrix} u^-_{\mathrm{sh}} \\ u^-_{\mathrm{sv}} \\ u^-_{\mathrm{p}} \end{pmatrix}, \qquad \boldsymbol{u} = \boldsymbol{u}^+ + \boldsymbol{u}^-.$$

The fields $\boldsymbol{u}^{\pm}$ are the generalized left and right going components (negative and positive z- direction) of the total field, respectively. Note that the y and z components of the total field $\boldsymbol{u}$ (i.e v and w) consist both of P and SV waves whereas the y component of the split fields $\boldsymbol{u}^{\pm}$ is an SV wave and the z component of the split field is a P wave. The wave splitting is defined by

$$\begin{pmatrix} \boldsymbol{u}^+ \\ \boldsymbol{u}^- \end{pmatrix} = \boldsymbol{\mathcal{S}} \begin{pmatrix} \boldsymbol{u} \\ \boldsymbol{\phi} \end{pmatrix},$$

where the matrix valued split operator $\boldsymbol{\mathcal{S}}$ is defined by

$$\boldsymbol{\mathcal{S}} = \frac{1}{2}\begin{pmatrix} 1 & 0 & 0 & -\frac{1}{Z_{\rm sh}}(\partial_t)^{-1} & 0 & 0 \\ 0 & 1 & 0 & 0 & \frac{1}{Z_{\rm sv}}(\partial_t)^{-1} & \frac{\alpha}{\rho}(\partial_t)^{-1} \\ 0 & 0 & 1 & 0 & \frac{\alpha}{\rho}(\partial_t)^{-1} & -\frac{1}{Z_{\rm p}}(\partial_t)^{-1} \\ 1 & 0 & 0 & \frac{1}{Z_{\rm sh}}(\partial_t)^{-1} & 0 & 0 \\ 0 & 1 & 0 & 0 & -\frac{1}{Z_{\rm sv}}(\partial_t)^{-1} & \frac{\alpha}{\rho}(\partial_t)^{-1} \\ 0 & 0 & 1 & 0 & \frac{\alpha}{\rho}(\partial_t)^{-1} & \frac{1}{Z_{\rm p}}(\partial_t)^{-1} \end{pmatrix},$$

where $(\partial_t)^{-1}$ denotes time integration $\int^t$. The functions $Z_{\rm sh}(z)$, $Z_{\rm sv}(z)$ and $Z_{\rm p}(z)$ are the modified impedances of the SH, SV and P modes and they read

$$\begin{aligned} Z_{\rm sh}(z) &= \rho(z)c_{\rm t}(z)\sqrt{1-\alpha^2 c_{\rm t}(z)^2} \\ Z_{\rm sv}(z) &= \rho(z)c_{\rm t}(z)\frac{1}{\sqrt{1-\alpha^2 c_{\rm t}(z)^2}} \\ Z_{\rm p}(z) &= \rho(z)c_{\rm l}(z)\frac{1}{\sqrt{1-\alpha^2 c_{\rm l}(z)^2}}. \end{aligned} \tag{3.8}$$

For a wave at normal incidence, i.e. $\alpha = 0$, the impedances in Eq. (3.8) are identical to the usual expressions for the impedances, cf. [10].

The split matrix $\boldsymbol{\mathcal{S}}$ is derived by diagonalizing the matrix $\boldsymbol{\mathcal{A}}$ in Eq. (3.7) for a homogeneous elastic medium. Thus, for a homogeneous elastic medium, the fields $\boldsymbol{u}^{\pm}$ are the physical left and right going components of the total field. In the inhomogeneous case, the splitting is still well defined but the fields $\boldsymbol{u}^{\pm}$ are generalized left and right going components of the total field.

The inverse of $\boldsymbol{\mathcal{S}}$ reads

$$\boldsymbol{\mathcal{S}}^{-1} = \begin{pmatrix} 1 & 0 & 0 & 1 & 0 & 0 \\ 0 & 1 & \frac{\alpha}{s_{\rm l}} & 0 & 1 & -\frac{\alpha}{s_{\rm l}} \\ 0 & -\frac{\alpha}{s_{\rm t}} & 1 & 0 & \frac{\alpha}{s_{\rm t}} & 1 \\ -Z_{\rm sh}\partial_t & 0 & 0 & Z_{\rm sh}\partial_t & 0 & 0 \\ 0 & Z_{\rm sv}\partial_t & 0 & 0 & -Z_{\rm sv}\partial_t & 0 \\ 0 & 0 & -Z_{\rm p}\partial_t & 0 & 0 & Z_{\rm p}\partial_t \end{pmatrix},$$

where $s_{\rm l}(z)$ and $s_{\rm t}(z)$ are the inverses of the wave speed of the longitudinal and transverse modes, respectively

$$\begin{aligned} s_{\rm t}(z) &= \frac{1}{c_{\rm t}(z)}\sqrt{1-\alpha^2 c_{\rm t}(z)^2} \\ s_{\rm l}(z) &= \frac{1}{c_{\rm l}(z)}\sqrt{1-\alpha^2 c_{\rm l}(z)^2}. \end{aligned}$$

The split fields $\boldsymbol{u}^{\pm}$ satisfy a system of first order hyperbolic equations that is equivalent to the wave equation (3.2)

$$\begin{aligned} \partial_z \begin{pmatrix} \boldsymbol{u}^+ \\ \boldsymbol{u}^- \end{pmatrix} &= \left((\partial_z \boldsymbol{\mathcal{S}})\,\boldsymbol{\mathcal{S}}^{-1} + \boldsymbol{\mathcal{S}}\boldsymbol{\mathcal{A}}\boldsymbol{\mathcal{S}}^{-1}\right)\begin{pmatrix} \boldsymbol{u}^+ \\ \boldsymbol{u}^- \end{pmatrix} \\ &\equiv \mathrm{Diag}\begin{pmatrix} -s_{\rm t}, & -s_{\rm t}, & -s_{\rm l}, & s_{\rm t}, & s_{\rm t}, & s_{\rm l} \end{pmatrix}\begin{pmatrix} \partial_t \boldsymbol{u}^+ \\ \partial_t \boldsymbol{u}^- \end{pmatrix} + \boldsymbol{\mathcal{B}}\begin{pmatrix} \boldsymbol{u}^+ \\ \boldsymbol{u}^- \end{pmatrix}. \end{aligned} \tag{3.9}$$

The 6×6 matrix valued operator $\boldsymbol{\mathcal{B}}$ consists of the coupling coefficients between the split fields. Diag () in Eq. (3.9) denotes the 6×6 diagonal matrix. In order to make the coupling coefficients from SV to P equal to the coupling coefficients from P to SV (except for the sign), the following scaling is performed

$$\boldsymbol{u}^{\pm} = \begin{pmatrix} u^{\pm}_{\rm sh} \\ u^{\pm}_{\rm sv} \\ u^{\pm}_{\rm p} \end{pmatrix} = \begin{pmatrix} \frac{1}{\sqrt{Z_{\rm sh}(z)}}\psi^{\pm}_{\rm sh} \\ \frac{1}{\sqrt{Z_{\rm sv}(z)}}\psi^{\pm}_{\rm sv} \\ \frac{1}{\sqrt{Z_{\rm p}(z)}}\psi^{\pm}_{\rm p} \end{pmatrix} = \text{Diag}\left(\frac{1}{\sqrt{Z_{\rm sh}(z)}}, \frac{1}{\sqrt{Z_{\rm sv}(z)}}, \frac{1}{\sqrt{Z_{\rm p}(z)}} \right) \boldsymbol{\psi}^{\pm}. \tag{3.10}$$

This scaling also makes $R_{\rm p\to sv} = -R_{\rm p\to sv}$ in Eq. (6.14). The new split fields $\boldsymbol{\psi}^{\pm}$ are inserted in Eq. (3.9) giving the equation

$$\partial_z \begin{pmatrix} \boldsymbol{\psi}^{+} \\ \boldsymbol{\psi}^{-} \end{pmatrix} \equiv \text{Diag}\left(-s_{\rm t}, \quad -s_{\rm t}, \quad -s_{\rm l}, \quad s_{\rm t}, \quad s_{\rm t}, \quad s_{\rm l} \right) \begin{pmatrix} \partial_t \boldsymbol{\psi}^{+} \\ \partial_t \boldsymbol{\psi}^{-} \end{pmatrix} + \boldsymbol{\mathcal{C}} \begin{pmatrix} \boldsymbol{\psi}^{+} \\ \boldsymbol{\psi}^{-} \end{pmatrix}, \tag{3.11}$$

where the 6×6 matrix valued operator $\boldsymbol{\mathcal{C}}$ reads

$$\begin{aligned} \boldsymbol{\mathcal{C}} &= \begin{pmatrix} \alpha_{\rm sh} + \tilde{\alpha}_{\rm sh}* & 0 & 0 & \beta_{\rm sh} + \tilde{\beta}_{\rm sh}* & 0 & 0 \\ 0 & & & 0 & & \\ 0 & \boldsymbol{\alpha}_{\rm psv} + \boldsymbol{\alpha}_{\rm psv}* & & 0 & \boldsymbol{\beta}_{\rm psv} + \boldsymbol{\beta}_{\rm psv}* & \\ \gamma_{\rm sh} + \gamma_{\rm sh}* & 0 & 0 & -\alpha_{\rm sh} - \alpha_{\rm sh}* & 0 & 0 \\ 0 & & & 0 & & \\ 0 & \boldsymbol{\gamma}_{\rm psv} + \boldsymbol{\gamma}_{\rm psv}* & & 0 & -\boldsymbol{\alpha}_{\rm psv} - \boldsymbol{\alpha}_{\rm psv}* & \end{pmatrix} \\ &= \begin{pmatrix} \alpha_{\rm sh} + \alpha_{\rm sh}* & 0 & 0 & & & \\ 0 & \alpha_{\rm sv} + \alpha_{\rm sv}* & \alpha_{\rm psv} + \alpha_{\rm psv}* & & & \\ 0 & -\alpha_{\rm psv} - \alpha_{\rm psv}* & \alpha_{\rm p} + \alpha_{\rm p}* & & & \\ \gamma_{\rm sh} + \gamma_{\rm sh}* & 0 & 0 & & & \\ 0 & \gamma_{\rm sv} + \gamma_{\rm sv}* & -\beta_{\rm psv} - \beta_{\rm psv}* & & & \\ 0 & \beta_{\rm psv} + \beta_{\rm psv}* & \gamma_{\rm p} + \gamma_{\rm p}* & & & \end{pmatrix} \\ &\qquad \begin{pmatrix} \beta_{\rm sh} + \beta_{\rm sh}* & 0 & 0 \\ 0 & \beta_{\rm sv} + \beta_{\rm sv}* & \beta_{\rm psv} + \beta_{\rm psv}* \\ 0 & -\beta_{\rm psv} - \beta_{\rm psv}* & \beta_{\rm p} + \beta_{\rm p}* \\ -\alpha_{\rm sh} - \alpha_{\rm sh}* & 0 & 0 \\ 0 & -\alpha_{\rm sv} - \alpha_{\rm sv}* & -\alpha_{\rm psv} - \alpha_{\rm psv}* \\ 0 & \alpha_{\rm psv} + \alpha_{\rm psv}* & -\alpha_{\rm p} - \alpha_{\rm p}* \end{pmatrix}. \end{aligned}$$

The boldface matrices are 2×2 matrices. The elements in the matrix $\boldsymbol{\mathcal{C}}$ are presented in appendix A. The index psv in Eq. (3.11) denotes the coupling between the SV and the P modes.

For a homogeneous elastic medium, the operator matrix $\boldsymbol{\mathcal{C}} = \boldsymbol{0}$ and the wave equation in Eq. (3.11) reads

$$\partial_z \begin{pmatrix} \boldsymbol{\psi}^{+} \\ \boldsymbol{\psi}^{-} \end{pmatrix} = \text{Diag}\left(-s_{\rm t}, \quad -s_{\rm t}, \quad -s_{\rm l}, \quad s_{\rm t}, \quad s_{\rm t}, \quad s_{\rm l} \right) \begin{pmatrix} \partial_t \boldsymbol{\psi}^{+} \\ \partial_t \boldsymbol{\psi}^{-} \end{pmatrix}.$$

In this case $u^{\pm}_{\rm sh}$ ($\psi^{\pm}_{\rm sh}$) and $u^{\pm}_{\rm sv}$ ($\psi^{\pm}_{\rm sv}$) propagate with the transverse velocity $s_{\rm t}^{-1}$ and $u^{\pm}_{\rm p}$ ($\psi^{\pm}_{\rm p}$) propagates with the longitudinal velocity $s_{\rm l}^{-1}$.

4 Wave propagators

In the direct and inverse problems, it is assumed that the incident transient plane wave $\boldsymbol{\psi}^{+}(0,t)$ has been generated in the region $z<0$, and impinges obliquely on the slab at $z=0$ and at time $t=0$. The incident field excites internal fields $\boldsymbol{\psi}^{\pm}(z',t)$ as well as reflected and transmitted fields. The wave propagators are linear operators that map the internal right going field $\boldsymbol{\psi}^{+}(z',t)$ at a position $z'>0$ to the internal left and right going fields $\boldsymbol{\psi}^{\pm}(z,t)$ at some other position $z>0$, cf. [20]. The 3×3 wave propagators matrices $\boldsymbol{\mathcal{P}}^{\pm}(z,z')$ are defined by

$$\begin{pmatrix} \psi^{\pm}_{\rm sh}\left(z,t+\tau_{\rm t}(z,z')\right) \\ \psi^{\pm}_{\rm sv}\left(z,t+\tau_{\rm l}(z,z')\right) \\ \psi^{\pm}_{\rm p}\left(z,t+\tau_{\rm l}(z,z')\right) \end{pmatrix} = \boldsymbol{\mathcal{P}}^{\pm}(z,z') \begin{pmatrix} \psi^{+}_{\rm sh}(z',t) \\ \psi^{+}_{\rm sv}(z',t) \\ \psi^{+}_{\rm p}(z',t) \end{pmatrix}. \tag{4.1}$$

In these definitions the travel time variables $\tau_{\rm t}(z,z')$ and $\tau_{\rm l}(z,z')$ of the transverse and the longitudinal modes respectively, are defined by

$$\begin{cases} \tau_{\rm t}(z,z') &= \displaystyle\int_{z'}^{z} s_{\rm t}(z'')\,dz'' = \int_{z'}^{z} \frac{1}{c_{\rm t}(z'')}\sqrt{1-\sin^2\theta\frac{c_{\rm t}(z'')^2}{c_0^2}}\;dz'' \\ \tau_{\rm l}(z,z') &= \displaystyle\int_{z'}^{z} s_{\rm l}(z'')\,dz'' = \int_{z'}^{z} \frac{1}{c_{\rm l}(z'')}\sqrt{1-\sin^2\theta\frac{c_{\rm l}(z'')^2}{c_0^2}}\;dz''. \end{cases}$$

Note that the travel time variable is the same for the SV and the P mode since they are coupled. The travel time $\tau_{\rm t}(z,z')$ and $\tau_{\rm l}(z,z')$ are the travel time for the wavefront from a point z to a point z' measured in the translated time variable for the transverse and the longitudinal modes, respectively, cf. Eq. (3.1).

In the definition of the propagators in Eq. (4.1), there are no restrictions on the relative magnitudes of z and z'. When $z'<z$ the propagators propagate the field $\boldsymbol{\psi}^{+}(z',t)$ forward in the z-direction and in time, and when $z'>z$, the propagation is backward in the z-direction and in time. The notation forward propagators and backward propagators are therefore adopted for $\boldsymbol{\mathcal{P}}^{\pm}(z,z')$ when $z'<z$ and $z'>z$ respectively. The definition of the wave propagators implies the following relations for positive z, z' and z''

$$\boldsymbol{\mathcal{P}}^{+}(z,z) = \boldsymbol{\mathcal{I}} = \text{identity operator} \tag{4.2}$$

$$\boldsymbol{\mathcal{P}}^{+}(z,z') = \boldsymbol{\mathcal{P}}^{+}(z,z'')\boldsymbol{\mathcal{P}}^{+}(z'',z') \tag{4.3}$$

$$\boldsymbol{\mathcal{P}}^{-}(z,z') = \boldsymbol{\mathcal{P}}^{-}(z,z)\boldsymbol{\mathcal{P}}^{+}(z,z'). \tag{4.4}$$

From eqs. (4.2) and (4.3) it is seen that

$$\boldsymbol{\mathcal{P}}^{+}(z,z')\boldsymbol{\mathcal{P}}^{+}(z',z) = \boldsymbol{\mathcal{I}}.$$

Therefore the inverse of $\boldsymbol{\mathcal{P}}^{+}(z,z')$ follows

$$\left(\boldsymbol{\mathcal{P}}^{+}(z,z')\right)^{-1} = \boldsymbol{\mathcal{P}}^{+}(z',z). \tag{4.5}$$

4.1 Explicit representations of the propagators

The explicit representations of the wave propagators follow from invariance under time translation and causality, cf. [20]

$$\begin{aligned}\boldsymbol{\mathcal{P}}^{+}(z,z')\boldsymbol{\psi}^{+}(z',t) &= \boldsymbol{a}(z,z')\begin{pmatrix}\psi^{+}_{\mathrm{sh}}(z',t)\\ \mathcal{S}(z,z')\psi^{+}_{\mathrm{sv}}(z',t)\\ \psi^{+}_{\mathrm{p}}(z',t)\end{pmatrix} + \left[\boldsymbol{P}^{+}(z,z',\cdot) * \boldsymbol{\psi}^{+}(z',\cdot)\right](t)\\ \boldsymbol{\mathcal{P}}^{-}(z,z')\boldsymbol{\psi}^{+}(z',t) &= \left[\boldsymbol{P}^{-}(z,z',\cdot) * \boldsymbol{\psi}^{+}(z',\cdot)\right](t),\end{aligned} \tag{4.6}$$

where the time-shift operator $\mathcal{S}(z,z')$ is defined by

$$\mathcal{S}(z,z')f(z',t) = f(z,t-\tau_{\mathrm{t}}(z,z')+\tau_{\mathrm{l}}(z,z')),$$

where $f(z',t<0)=0$, due to causality. The propagator kernels, $\boldsymbol{P}^{\pm}(z,z',t)$, are 3×3 matrices

$$\boldsymbol{P}^{\pm}(z,z',t) = \begin{pmatrix} P^{\pm}_{\mathrm{sh}}(z,z',t) & 0 & 0\\ 0 & P^{\pm}_{\mathrm{sv}}(z,z',t) & P^{\pm}_{\mathrm{p}\to\mathrm{sv}}(z,z',t)\\ 0 & P^{\pm}_{\mathrm{sv}\to\mathrm{p}}(z,z',t) & P^{\pm}_{\mathrm{p}}(z,z',t)\end{pmatrix},$$

where $P^{\pm}_{\mathrm{p}\to\mathrm{sv}}$ denote the coupling from the P mode to the SV mode and $P^{\pm}_{\mathrm{sv}\to\mathrm{p}}$ the coupling from the SV mode to the P mode. The attenuation of the wavefront, $\boldsymbol{a}(z,z')$, from a point z' to a point z is a diagonal 3×3 matrix

$$\boldsymbol{a}(z,z') = \mathrm{Diag}\left(\ a_{\mathrm{sh}}(z,z'),\quad a_{\mathrm{sv}}(z,z'),\quad a_{\mathrm{p}}(z,z')\ \right).$$

The time-shift operator $\mathcal{S}(z,z')$ is applied to the directly transmitted part of the SV wave since the same wavefront time has to be used for the coupled P and SV modes and since the SV wave travels with the speed s_{t}^{-1} rather than s_{l}^{-1}.

The representations in Eq. (4.6) imply the following boundary values of the propagator kernels for a slab $0\le z\le L$

$$\left\{\begin{array}{rcl} \boldsymbol{P}^{-}(0,0,t) = \boldsymbol{R}(t) &=& \begin{pmatrix} R_{\mathrm{sh}}(t) & 0 & 0\\ 0 & R_{\mathrm{sv}}(t) & R_{\mathrm{p}\to\mathrm{sv}}(t)\\ 0 & R_{\mathrm{sv}\to\mathrm{p}}(t) & R_{\mathrm{p}}(t)\end{pmatrix}\\ \boldsymbol{P}^{+}(0,L,t) = \boldsymbol{T}(t) &=& \begin{pmatrix} T_{\mathrm{sh}}(t) & 0 & 0\\ 0 & T_{\mathrm{sv}}(t) & T_{\mathrm{p}\to\mathrm{sv}}(t)\\ 0 & T_{\mathrm{sv}\to\mathrm{p}}(t) & T_{\mathrm{p}}(t)\end{pmatrix},\end{array}\right. \tag{4.7}$$

where $\boldsymbol{R}(t)$ is the reflection matrix kernel and $\boldsymbol{T}(t)$ the transmission matrix kernel of the slab. For an incident delta pulse, the reflection kernel $\boldsymbol{R}(t)$ is the reflected response of the slab and $\boldsymbol{T}(t)$ is the transmitted scattered response. Since the P and SV modes are coupled for oblique excitation, an incident P wave gives rise to a reflected P wave through the kernel $R_{\mathrm{p}}(t)$ and a reflected SV wave through the kernel $R_{\mathrm{p}\to\mathrm{sv}}(t)$. As mentioned earlier, the reflection kernels $R_{\mathrm{p}\to\mathrm{sv}}(t)$ and $R_{\mathrm{sv}\to\mathrm{p}}(t)$ are identical except for the sign because of the scaling in Eq. (3.10).

From Eq. (4.2) and the propagator representation (4.6), it is seen that the propagator kernel $\boldsymbol{P}^+(z,z',t)$ is related to its inverse propagator kernel $\boldsymbol{P}^+(z',z,t)$ in Eq. (4.3) via Volterra equations of the second kind. For the SH mode, the Volterra equation reads

$$a_{\mathrm{sh}}(z',z)P^+_{\mathrm{sh}}(z,z',t) + a_{\mathrm{sh}}(z,z')P^+_{\mathrm{sh}}(z',z,t) + \left[P^+_{\mathrm{sh}}(z,z',\cdot) * P^+_{\mathrm{sh}}(z',z,\cdot)\right](t) = 0. \tag{4.8}$$

The system of coupled Volterra equations for the P-SV modes reads

$$\begin{aligned}\left[\boldsymbol{P}^+_{\mathrm{psv}}(z,z',\cdot) * \boldsymbol{P}^+_{\mathrm{psv}}(z',z,\cdot)\right](t) + \begin{pmatrix} a_{\mathrm{sv}}(z,z')\mathcal{S}(z,z') & 0 \\ 0 & a_{\mathrm{p}}(z,z') \end{pmatrix} \boldsymbol{P}^+_{\mathrm{psv}}(z,z',t) \\ + \left(\begin{pmatrix} a_{\mathrm{sv}}(z',z)\mathcal{S}(z',z) & 0 \\ 0 & a_{\mathrm{p}}(z',z) \end{pmatrix} \left(\boldsymbol{P}^+_{\mathrm{psv}}(z',z,t)\right)^T \right)^T = 0, \end{aligned} \tag{4.9}$$

where

$$\boldsymbol{P}^{\pm}_{\mathrm{psv}}(z,z',t) = \begin{pmatrix} P^{\pm}_{\mathrm{sv}}(z,z',t) & P^{\pm}_{\mathrm{p}\to\mathrm{sv}}(z,z',t) \\ P^{\pm}_{\mathrm{sv}\to\mathrm{p}}(z,z',t) & P^{\pm}_{\mathrm{p}}(z,z',t) \end{pmatrix}.$$

The kernel $\boldsymbol{P}^+(z,z',t)$ is uniquely given by the kernel $\boldsymbol{P}^+(z',z,t)$ and vice versa, since Volterra equations of the second kind have unique solutions. Hence, the inverse operator $\left(\boldsymbol{\mathcal{P}}^+(z,z')\right)^{-1}$ in Eq. (4.5) exists.

5 Relations to other techniques

There are two methods that are closely related to the propagator method: the imbedding method and the Green functions technique. The relations between these methods are discussed in this section. Historically, the imbedding method was first developed, followed by the Green functions technique and finally the wave propagator method. A modification of the Green functions technique is the compact Green function technique and this approach is also discussed.

5.1 The Green function technique

In the Green function approach, see [13, 17, 23, 24], Green operators $\boldsymbol{\mathcal{G}}^{\pm}(z)$ are introduced that map the incident field $\boldsymbol{\psi}^+(0,t)$ at $z=0$ ($z'=0$ in Eq. (4.6)) to the internal split fields $\boldsymbol{\psi}^{\pm}(z,t)$ as

$$\begin{pmatrix} \psi^{\pm}_{\mathrm{sh}}\left(z,t+\tau_{\mathrm{t}}(z,0)\right) \\ \psi^{\pm}_{\mathrm{sv}}\left(z,t+\tau_{\mathrm{l}}(z,0)\right) \\ \psi^{\pm}_{\mathrm{p}}\left(z,t+\tau_{\mathrm{l}}(z,0)\right) \end{pmatrix} = \boldsymbol{\mathcal{G}}^{\pm}(z) \begin{pmatrix} \psi^{+}_{\mathrm{sh}}(0,t) \\ \psi^{+}_{\mathrm{sv}}(0,t) \\ \psi^{+}_{\mathrm{p}}(0,t) \end{pmatrix}. \tag{5.1}$$

By comparing eqs. (5.1) and (4.1), the relation between the Green operators and the wave propagators and the relation between the Green kernels and the propagator kernels follow

$$\begin{aligned} \boldsymbol{\mathcal{G}}^{\pm}(z) &= \boldsymbol{\mathcal{P}}^{\pm}(z,0) \\ \boldsymbol{G}^{\pm}(z,t) &= \boldsymbol{P}^{\pm}(z,0,t). \end{aligned}$$

Thus, the Green operators $\boldsymbol{\mathcal{G}}^{\pm}(z)$ are the forward wave propagators $\boldsymbol{\mathcal{P}}^{\pm}(z,z'),\ z'<z$ for the special case $z'=0$. The equations, initial values and jump conditions for the Green kernels $\boldsymbol{G}^{\pm}(z,t)$ are derived by varying the coordinate z in Eq. (4.6). These results are presented in Section 6. In order to solve the Green kernel equations uniquely for a slab $0\leq z\leq L$, the following boundary conditions are needed

$$\begin{aligned}\boldsymbol{G}^{+}(0,t) &= \mathbf{0}\\ \boldsymbol{G}^{-}(L^{+},t) &= \mathbf{0},\end{aligned} \tag{5.2}$$

where $\mathbf{0}$ is the 3×3 null-matrix. The first boundary condition is obvious from Eq. (4.6) and the second follows since the medium is homogeneous and elastic for $z>L$ and thus no field is scattered backwards for $z>L$.

5.2 The "compact" Green function technique

In the "compact" Green function approach, see [15, 26], the Green operators $\boldsymbol{\mathcal{G}}^{c\pm}(z)$ map the transmitted field $\boldsymbol{\psi}^{+}(L,t)$ at $z=L$ to the internal split fields $\boldsymbol{\psi}^{\pm}(z,t)$ as

$$\begin{pmatrix}\psi^{\pm}_{\mathrm{sh}}\left(z,t+\tau_{\mathrm{t}}(z,L)\right)\\ \psi^{\pm}_{\mathrm{sv}}\left(z,t+\tau_{\mathrm{l}}(z,L)\right)\\ \psi^{\pm}_{\mathrm{p}}\left(z,t+\tau_{\mathrm{l}}(z,L)\right)\end{pmatrix}=\boldsymbol{\mathcal{G}}^{c\pm}(z)\begin{pmatrix}\psi^{+}_{\mathrm{sh}}(L,t)\\ \psi^{+}_{\mathrm{sv}}(L,t)\\ \psi^{+}_{\mathrm{p}}(L,t)\end{pmatrix}. \tag{5.3}$$

Thus, the operators $\boldsymbol{\mathcal{G}}^{c\pm}(z)$ are the backward wave propagators $\boldsymbol{\mathcal{P}}^{\pm}(z,z'),\ z'>z$ for the special case $z'=L$. The relations between these Green operators and the wave propagators follow by comparing eqs. (5.3) and (4.1)

$$\begin{aligned}\boldsymbol{\mathcal{G}}^{c\pm}(z) &= \boldsymbol{\mathcal{P}}^{\pm}(z,L)\\ \boldsymbol{G}^{c\pm}(z,t) &= \boldsymbol{P}^{\pm}(z,L,t).\end{aligned}$$

The equations, initial values and jump conditions for the compact Green kernels $\boldsymbol{G}^{c\pm}(z,t)$ are the same as for the usual Green kernels, see Section 6. For an elastic slab $0\leq z\leq L$, it turns out that the kernels $\boldsymbol{G}^{c\pm}(z,t)$ have compact support in the time interval $0<t<2\tau_{\mathrm{l}}(z,L)$ which explains the notation compact Green functions, cf. [15]. For a general dispersive slab, the kernels $\boldsymbol{G}^{c\pm}(z,t)$ do not have compact support in time and the name compact Green functions is somewhat misleading. The compactness of the kernels can be utilized to determine two material parameters from the reflection and transmission kernels for a field normally incident from one side of a non-dispersive slab, cf. [26]. The compact Green functions are also suitable for signal restoration, cf. [25]

Since the usual and "compact" Green operators are forward and backward wave propagators for the slab $0\leq z\leq L$ respectively, the relation between the kernels $\boldsymbol{G}^{+}(z=L,t)$ and $\boldsymbol{G}^{c+}(z=0,t)$ are given by eqs. (4.8) and (4.9). Similarly, the relation between the kernels $\boldsymbol{G}^{-}(z=0,t)$ and $\boldsymbol{G}^{c-}(z=L,t)$ is found from Eq. (4.4) for $z=0$ and $z'=L$. The boundary conditions for the compact Green kernels are

$$\begin{aligned}\boldsymbol{G}^{c+}(L,t) &= \mathbf{0}\\ \boldsymbol{G}^{c-}(L^{+},t) &= \mathbf{0},\end{aligned} \tag{5.4}$$

where $\mathbf{0}$ is the 3×3 null-matrix.

5.3 The imbedding method

The wave operators in the imbedding method are the reflection operator $\boldsymbol{\mathcal{R}}(z')$ and the transmission operator $\boldsymbol{\mathcal{T}}(z')$ for a subslab $[z', L]$ imbedded in a slab $[0, L]$, see [2, 8, 9, 11, 19]. The relation between the operators $\boldsymbol{\mathcal{R}}(z')$, $\boldsymbol{\mathcal{T}}(z')$ and the wave propagator operators are

$$\begin{aligned} \boldsymbol{\mathcal{R}}(z') &= \boldsymbol{\mathcal{P}}^-(z', z') \\ \boldsymbol{\mathcal{T}}(z') &= \boldsymbol{\mathcal{P}}^+(L, z'). \end{aligned}$$

Thus, the transmission operator $\boldsymbol{\mathcal{T}}(z')$ is the forward wave propagator $\boldsymbol{\mathcal{P}}^+(z, z')$ for the special case $z = L$ that map the right going field $\boldsymbol{\psi}^+(z', t)$ to the transmitted field $\boldsymbol{\psi}^+(L, t)$. Note that $\boldsymbol{\mathcal{T}}(z')$ is the inverse of the compact Green operator $\boldsymbol{\mathcal{G}}^{c+}(z', t)$, cf. Eq. (4.5), and thus, the corresponding kernels are related through eqs. (4.8) and (4.9). The reflection and transmission kernels in the imbedding method are related to the propagator kernels as

$$\begin{aligned} \boldsymbol{R}(z', t) &= \boldsymbol{P}^-(z', z', t) \\ \boldsymbol{T}(z', t) &= \boldsymbol{P}^+(L, z', t). \end{aligned}$$

Note that $\boldsymbol{R}(z', t)$ is antisymmetric, i.e. $R_{\mathrm{p}\to\mathrm{sv}}(z', t) = -R_{\mathrm{sv}\to\mathrm{p}}(z', t)$, cf. Eq. (6.14). The equations for the reflection and transmission kernels, $\boldsymbol{R}(z', t)$ and $\boldsymbol{T}(z', t)$, are derived by varying the coordinate z' in Eq. (4.6). The derivation is found in the next section. In order to solve the imbedding equations uniquely, the following boundary conditions are needed

$$\begin{aligned} \boldsymbol{T}(L, t) &= \boldsymbol{0} \\ \boldsymbol{R}(L^+, t) &= \boldsymbol{0}, \end{aligned} \tag{5.5}$$

where $\boldsymbol{0}$ is the 3×3 null-matrix.

6 The equations for the propagator kernels

In this section, the equations and the initial values for the propagator kernels are derived by differentiating both sides of the definition of the wave propagators in Eq. (4.1) with respect to the coordinate z or z'. When the coordinate z is varied while z' is kept constant, this set of equations is related to the one obtained in the Green functions approach. For $z' = 0$, this set of equations is identical to the equations obtained in the Green functions approach and for $z' = L$, the equations for the "compact" Green functions are obtained. The other set of equations is derived by varying the coordinate z' and is related to the imbedding equations.

6.1 The equations related to the Green kernel equations

The differentiation with respect to z of the left hand side of Eq. (4.1) gives

$$\begin{aligned} \frac{d}{dz} \begin{pmatrix} \boldsymbol{\psi}^+ \\ \boldsymbol{\psi}^- \end{pmatrix} (z, t + \tau_{(\cdot)}(z, z')) &= \begin{pmatrix} \partial_z \boldsymbol{\psi}^+ \\ \partial_z \boldsymbol{\psi}^- \end{pmatrix} (z, t + \tau_{(\cdot)}(z, z')) \\ &+ \mathrm{Diag} \begin{pmatrix} s_{\mathrm{t}}, & s_{\mathrm{l}}, & s_{\mathrm{l}}, & s_{\mathrm{t}}, & s_{\mathrm{l}}, & s_{\mathrm{l}} \end{pmatrix} \begin{pmatrix} \partial_t \boldsymbol{\psi}^+ \\ \partial_t \boldsymbol{\psi}^- \end{pmatrix} (z, t + \tau_{(\cdot)}(z, z')). \end{aligned}$$

The dynamics in Eq. (3.11) eliminate the partial derivatives with respect to z and the representation in Eq. (4.6) eliminates $\boldsymbol{\psi}^{\pm}(z, t+\tau_{(\cdot)}(z,z'))$ in this equation. Thus

$$\begin{aligned}\frac{d}{dz}\begin{pmatrix}\boldsymbol{\psi}^{+}\\ \boldsymbol{\psi}^{-}\end{pmatrix}(z,t+\tau_{(\cdot)}(z,z')) &= \boldsymbol{\mathcal{C}}\begin{pmatrix}\boldsymbol{\mathcal{P}}^{+}(z,z')\boldsymbol{\psi}^{+}(z',t)\\ \boldsymbol{\mathcal{P}}^{-}(z,z')\boldsymbol{\psi}^{+}(z',t)\end{pmatrix}\\ &+\operatorname{Diag}\begin{pmatrix}0, & -s_{\mathrm{t}}+s_{\mathrm{l}}, & 0, & 2s_{\mathrm{t}}, & s_{\mathrm{t}}+s_{\mathrm{l}}, & 2s_{\mathrm{l}}\end{pmatrix}\partial_t\begin{pmatrix}\boldsymbol{\mathcal{P}}^{+}(z,z')\boldsymbol{\psi}^{+}(z',t)\\ \boldsymbol{\mathcal{P}}^{-}(z,z')\boldsymbol{\psi}^{+}(z',t)\end{pmatrix}.\end{aligned} \tag{6.1}$$

By utilizing Eq. (4.6) the derivative with respect to z of the right hand side of Eq. (4.1) reads

$$\begin{aligned}\frac{d}{dz}\begin{pmatrix}\boldsymbol{\mathcal{P}}^{+}(z,z')\boldsymbol{\psi}^{+}(z',t)\\ \boldsymbol{\mathcal{P}}^{-}(z,z')\boldsymbol{\psi}^{+}(z',t)\end{pmatrix} &= \begin{pmatrix}\partial_z\boldsymbol{a}(z,z')\begin{pmatrix}\psi^{+}_{\mathrm{sh}}(z',t)\\ \mathcal{S}(z,z')\psi^{+}_{\mathrm{sv}}(z',t)\\ \psi^{+}_{\mathrm{p}}(z',t)\end{pmatrix}\\ \mathbf{0}\end{pmatrix}\\ &-(s_{\mathrm{t}}-s_{\mathrm{l}})\begin{pmatrix}\begin{pmatrix}0\\ a_{\mathrm{sv}}(z,z')\mathcal{S}(z,z')\partial_t\psi^{+}_{\mathrm{sv}}(z',t)\\ 0\end{pmatrix}\\ \mathbf{0}\end{pmatrix}\\ &+\begin{bmatrix}\partial_z\boldsymbol{P}^{+}(z,z',\cdot)*\boldsymbol{\psi}^{+}(z',\cdot)\\ \partial_z\boldsymbol{P}^{-}(z,z',\cdot)*\boldsymbol{\psi}^{+}(z',\cdot)\end{bmatrix}(t).\end{aligned} \tag{6.2}$$

where $\mathbf{0}$ is the 3×1 null-vector. When the right hand sides of eqs. (6.1) and (6.2) are set equal to each other, a system of equations in terms of the field $\boldsymbol{\psi}^{+}(z',t)$ is obtained. The incident field $\boldsymbol{\psi}^{+}(0,t)$ is an arbitrary incident field, and since the backward propagator $\boldsymbol{\mathcal{P}}^{+}(0,z')$ exists, the internal field $\boldsymbol{\psi}^{+}(z',t)$ is an arbitrary incident field and the system of equations for the kernels of the SH mode and the coupled system for the SV and P modes are obtained. Equations (6.1) and (6.2) also give the initial values for the propagator kernels, the values of the discontinuities in the propagator kernels and the equation for the attenuation factor. The system of equations and the initial condition for the kernels $P^{\pm}_{\mathrm{sh}}(z,z',t)$ read

$$\begin{aligned}&\partial_z\begin{pmatrix}P^{+}_{\mathrm{sh}}(z,z',t)\\ P^{-}_{\mathrm{sh}}(z,z',t)\end{pmatrix}-2s_{\mathrm{t}}(z)\partial_t\begin{pmatrix}0\\ P^{-}_{\mathrm{sh}}(z,z',t)\end{pmatrix}\\ =\;&\begin{pmatrix}\alpha_{\mathrm{sh}}(z) & \beta_{\mathrm{sh}}(z)\\ \gamma_{\mathrm{sh}}(z) & -\alpha_{\mathrm{sh}}(z)\end{pmatrix}\begin{pmatrix}P^{+}_{\mathrm{sh}}(z,z',t)\\ P^{-}_{\mathrm{sh}}(z,z',t)\end{pmatrix}+\begin{pmatrix}a_{\mathrm{sh}}(z,z')\alpha_{\mathrm{sh}}(z,t)\\ a_{\mathrm{sh}}(z,z')\gamma_{\mathrm{sh}}(z,t)\end{pmatrix}.\\ &+\begin{pmatrix}\alpha_{\mathrm{sh}}(z,\cdot)* & \beta_{\mathrm{sh}}(z,\cdot)*\\ \gamma_{\mathrm{sh}}(z,\cdot)* & -\alpha_{\mathrm{sh}}(z,\cdot)*\end{pmatrix}\begin{bmatrix}P^{+}_{\mathrm{sh}}(z,z',\cdot)\\ P^{-}_{\mathrm{sh}}(z,z',\cdot)\end{bmatrix}(t)\end{aligned}$$

$$P^{-}_{\mathrm{sh}}(z,z',0)=-\frac{1}{2}\frac{a_{\mathrm{sh}}(z,z')}{s_{\mathrm{t}}(z)}\gamma_{\mathrm{sh}}(z). \tag{6.3}$$

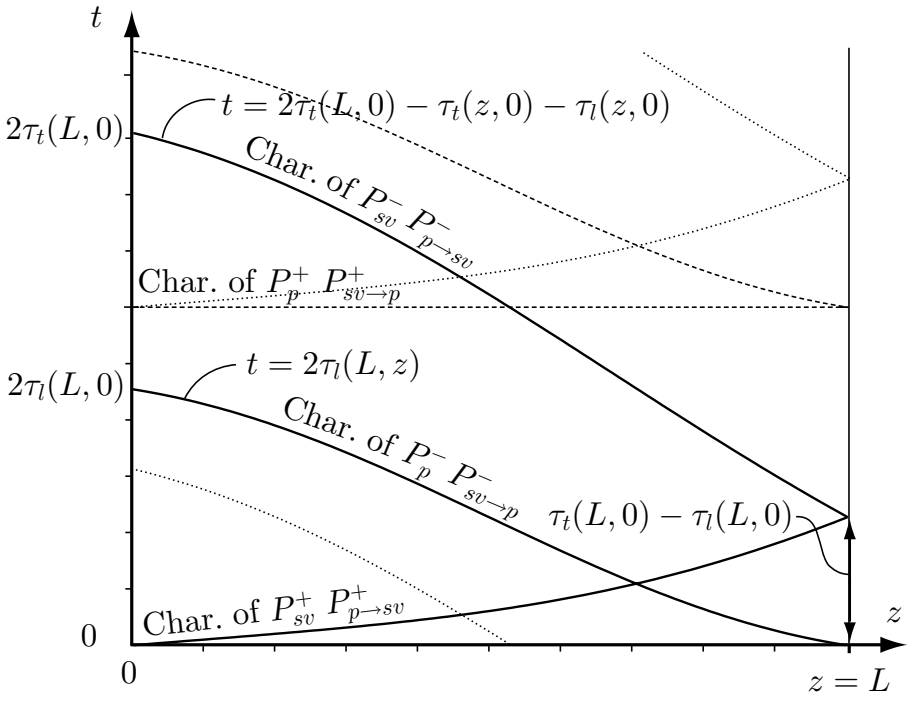

Figure 2: Some characteristic lines of the coupled propagator kernels $P^{\pm}(z,0,t)$ and $P^{\pm}(z,L,t)$, i.e the Green kernels for a slab $0 \leq z \leq L$.

The coupled system of equations for the propagator kernels $\boldsymbol{P}^+_{\rm psv}(z,z',t)$ of the SV and P modes read

$$\begin{aligned}
&\partial_z \begin{pmatrix} P^+_{\rm sv} & P^+_{\rm p\to sv} \\ P^+_{\rm sv\to p} & P^+_{\rm p} \\ P^-_{\rm sv} & P^-_{\rm p\to sv} \\ P^-_{\rm sv\to p} & P^-_{\rm p} \end{pmatrix} - \partial_t \begin{pmatrix} (s_{\rm l}-s_{\rm t})\,P^+_{\rm sv} & (s_{\rm l}-s_{\rm t})\,P^+_{\rm p\to sv} \\ 0 & 0 \\ (s_{\rm t}+s_{\rm l})\,P^-_{\rm sv} & (s_{\rm t}+s_{\rm l})\,P^-_{\rm p\to sv} \\ 2s_{\rm l}P^-_{\rm sv\to p} & 2s_{\rm l}P^-_{\rm p} \end{pmatrix} \qquad (6.4)\\
&= \begin{pmatrix} \boldsymbol{\alpha}_{\rm psv} + \boldsymbol{\alpha}_{\rm psv}* & \boldsymbol{\beta}_{\rm psv} + \boldsymbol{\beta}_{\rm psv}* \\ \boldsymbol{\gamma}_{\rm psv} + \boldsymbol{\gamma}_{\rm psv}* & -\boldsymbol{\alpha}_{\rm psv} - \boldsymbol{\alpha}_{\rm psv}* \end{pmatrix} \begin{pmatrix} \boldsymbol{P}^+_{\rm psv} \\ \boldsymbol{P}^-_{\rm psv} \end{pmatrix} \\
&+ \begin{pmatrix} a_{\rm sv}(z,z')\mathcal{S}(z,z')\alpha_{\rm sv}(z,t) & a_{\rm p}(z,z')\alpha_{\rm psv}(z,t) \\ -a_{\rm sv}(z,z')\mathcal{S}(z,z')\alpha_{\rm psv}(z,t) & a_{\rm p}(z,z')\alpha_{\rm p}(z,t) \\ a_{\rm sv}(z,z')\mathcal{S}(z,z')\gamma_{\rm sv}(z,t) & -a_{\rm p}(z,z')\beta_{\rm psv}(z,t) \\ a_{\rm sv}(z,z')\mathcal{S}(z,z')\beta_{\rm psv}(z,t) & a_{\rm p}(z,z')\gamma_{\rm p}(z,t) \end{pmatrix}.
\end{aligned}$$

The initial values for the $P^{\pm}_{\rm p\to sv}$ and $P^+_{\rm p}$ kernels read

$$\left\{ \begin{aligned}
P^+_{\rm p\to sv}(z,z',0) &= \frac{a_{\rm p}(z,z')}{s_{\rm t}(z)-s_{\rm l}(z)}\alpha_{\rm psv}(z) \\
P^-_{\rm p\to sv}(z,z',0) &= \frac{a_{\rm p}(z,z')}{s_{\rm l}(z)+s_{\rm t}(z)}\beta_{\rm psv}(z) \\
P^-_{\rm p}(z,z',0) &= -\frac{1}{2}\frac{a_{\rm p}(z,z')}{s_{\rm l}(z)}\gamma_{\rm p}(z).
\end{aligned} \right. \qquad (6.5)$$

The wavefront time used in the representations in Eq. (4.6) implies that $t = 0$ when the wavefront of the P wave arrives at a point z. Since the SV wave travels at a lower wavefront speed, it has not arrived at time $t = 0$, and hence the initial values for the SV wave read

$$\begin{cases} P^{+}_{\mathrm{sv}}(z,z',0) & = 0 \\ P^{-}_{\mathrm{sv}}(z,z',0) & = 0 \\ P^{-}_{\mathrm{sv}\to\mathrm{p}}(z,z',0) & = 0. \end{cases} \tag{6.6}$$

From the left hand side of (6.4), the characteristics of the kernels $P^{\pm}_{\mathrm{sv}}$, $P^{\pm}_{\mathrm{sv}\to\mathrm{p}}$, $P^{\pm}_{\mathrm{p}}$ and $P^{\pm}_{\mathrm{p}\to\mathrm{sv}}$ are easily obtained. Some of the corresponding characteristic lines for a slab $0 \le z \le L$ are presented in Figure 2.

The kernels P^{-}_{sv}, $P^{-}_{\mathrm{sv}\to\mathrm{p}}$ and $P^{+}_{\mathrm{sv}\to\mathrm{p}}$ have jump discontinuities along the characteristic line $t = \tau_{\mathrm{t}}(z,0) - \tau_{\mathrm{l}}(z,0)$ for a slab $0 \le z \le L$, see Figure 2. The wavefront of the SV mode propagates along this characteristic line and initiates a P wave through the kernels $P^{-}_{\mathrm{sv}\to\mathrm{p}}$ and $P^{+}_{\mathrm{sv}\to\mathrm{p}}$. Thus, the jump discontinuity in P^{-}_{sv} is the initial value for the directly propagating SV wave. For a wave at normal incidence, this discontinuity is equal to the initial value for the SH wave in Eq. (6.3). The jump conditions for the SV and P modes are obtained by integrating the propagator kernels along their characteristics, see [26]

$$\begin{cases} \left[P^{-}_{\mathrm{sv}}(z,z',t)\right]_{t=\tau_{\mathrm{t}}(z,0)-\tau_{\mathrm{l}}(z,0)} & = -\dfrac{1}{2}\dfrac{a_{\mathrm{sv}}(z,z')}{s_{\mathrm{t}}(z)}\gamma_{\mathrm{sv}}(z) \\ \left[P^{+}_{\mathrm{sv}\to\mathrm{p}}(z,z',t)\right]_{t=\tau_{\mathrm{t}}(z,0)-\tau_{\mathrm{l}}(z,0)} & = \dfrac{a_{\mathrm{sv}}(z,z')}{s_{\mathrm{t}}(z)-s_{\mathrm{l}}(z)}\alpha_{\mathrm{psv}}(z) \\ \left[P^{-}_{\mathrm{sv}\to\mathrm{p}}(z,z',t)\right]_{t=\tau_{\mathrm{t}}(z,0)-\tau_{\mathrm{l}}(z,0)} & = -\dfrac{a_{\mathrm{sv}}(z,z')}{s_{\mathrm{l}}(z)+s_{\mathrm{t}}(z)}\beta_{\mathrm{psv}}(z), \end{cases} \tag{6.7}$$

where $[f(z,z',t)]_{t=t_0} = f(z,z',t_0^+) - f(z,z',t_0^-)$.

The equation for the attenuation $\boldsymbol{a}(z,z')$ also follows from eqs. (6.1) and (6.2)

$$\mathrm{Diag}\left(\ \alpha_{\mathrm{sh}}(z,z'),\ \ \alpha_{sv}(z,z'),\ \ \alpha_{\mathrm{p}}(z,z')\ \right)\boldsymbol{a}(z,z') = \partial_z \boldsymbol{a}(z,z'). \tag{6.8}$$

The initial value $\boldsymbol{a}(z,z) = \mathrm{Diag}\left(\ 1,\ \ 1,\ \ 1\ \right)$, is implied by the representation in Eq. (4.6), and hence the solution of Eq. (6.8) reads

$$\begin{cases} a_{\mathrm{sh}}(z,z') & = \exp\left\{\displaystyle\int_{z'}^{z}\alpha_{\mathrm{sh}}(z'')dz''\right\} & = \exp\left\{\dfrac{1}{2}\displaystyle\int_{z'}^{z}\rho(z'')\dfrac{G_t(z'',0)}{Z_{\mathrm{sh}}(z'')G(z'',0)}dz''\right\} \\ a_{\mathrm{sv}}(z,z') & = \exp\left\{\displaystyle\int_{z'}^{z}\alpha_{\mathrm{sv}}(z'')dz''\right\} & = \exp\left\{\dfrac{1}{2}\displaystyle\int_{z'}^{z}Z_{\mathrm{sv}}(z'')\dfrac{G_t(z'',0)}{G(z'',0)^2}dz''\right\} \\ a_{\mathrm{p}}(z,z') & = \exp\left\{\displaystyle\int_{z'}^{z}\alpha_{\mathrm{p}}(z'')dz''\right\} & = \exp\left\{\dfrac{1}{2}\displaystyle\int_{z'}^{z}Z_{\mathrm{p}}(z'')\dfrac{E_t(z'',0)}{E(z'',0)^2}dz''\right\}. \end{cases} \tag{6.9}$$

6.2 The imbedding equations

The differentiation with respect to z' of the left hand side of Eq. (4.1) with $z = z'$ in $\boldsymbol{\psi}^-$ gives

$$\frac{d}{dz'}\begin{pmatrix} \boldsymbol{\psi}^+(z,t+\tau_{(\cdot)}(z,z')) \\ \boldsymbol{\psi}^-(z',t+\tau_{(\cdot)}(z',z')) \end{pmatrix} = \begin{pmatrix} -\mathrm{Diag}\begin{pmatrix} s_\mathrm{t}, & s_\mathrm{l}, & s_\mathrm{l} \end{pmatrix}\partial_t \boldsymbol{\mathcal{P}}^+(z,z')\boldsymbol{\psi}^+(z',t) \\ \partial_{z'}\boldsymbol{\psi}^-(z',t) \end{pmatrix}. \tag{6.10}$$

The dynamics in Eq. (3.11) eliminates $\partial_{z'}\boldsymbol{\psi}^-$ and Eq. (4.6) eliminates $\boldsymbol{\psi}^-(z',t) = \boldsymbol{\mathcal{P}}^-(z',z')\boldsymbol{\psi}^+(z',t)$. The derivative with respect to z' of the right hand side of Eq. (4.1) can, by using Eq. (4.6), be written as

$$\begin{aligned}
\frac{d}{dz'}\begin{pmatrix} \boldsymbol{\mathcal{P}}^+(z,z')\boldsymbol{\psi}^+(z',t) \\ \boldsymbol{\mathcal{P}}^-(z',z')\boldsymbol{\psi}^+(z',t) \end{pmatrix} &= \begin{pmatrix} \partial_{z'}\boldsymbol{a}(z,z')\begin{pmatrix} \psi^+_\mathrm{sh}(z',t) \\ \mathcal{S}(z,z')\psi^+_\mathrm{sv}(z',t) \\ \psi^+_\mathrm{p}(z',t) \end{pmatrix} \\ \mathbf{0} \end{pmatrix} \\
&+ (s_\mathrm{t}-s_\mathrm{l})\begin{pmatrix} \begin{pmatrix} 0 \\ a_\mathrm{sv}(z,z')\mathcal{S}(z,z')\partial_t\psi^+_\mathrm{sv}(z',t) \\ 0 \end{pmatrix} \\ \mathbf{0} \end{pmatrix} \\
&+ \begin{pmatrix} \boldsymbol{a}(z,z')\begin{pmatrix} \partial_{z'}\psi^+_\mathrm{sh}(z',t) \\ \mathcal{S}(z,z')\partial_{z'}\psi^+_\mathrm{sv}(z',t) \\ \partial_{z'}\psi^+_\mathrm{p}(z',t) \end{pmatrix} \\ \mathbf{0} \end{pmatrix} \\
&+ \begin{bmatrix} \partial_{z'}\boldsymbol{P}^+(z,z',\cdot) * \boldsymbol{\psi}^+(z',\cdot) \\ \partial_{z'}\boldsymbol{P}^-(z',z',\cdot) * \boldsymbol{\psi}^+(z',\cdot) \end{bmatrix}(t) + \begin{bmatrix} \boldsymbol{P}^+(z,z',\cdot) * \partial_{z'}\boldsymbol{\psi}^+(z',\cdot) \\ \boldsymbol{P}^-(z',z',\cdot) * \partial_{z'}\boldsymbol{\psi}^+(z',\cdot) \end{bmatrix}(t),
\end{aligned} \tag{6.11}$$

where the dynamics in (3.11) is used to eliminate $\partial_{z'}\boldsymbol{\psi}^+$. Putting eqs. (6.10) and (6.11) equal results in a system of equations in terms of $\boldsymbol{\psi}^+(z',t)$ and since this is an arbitrary field, the system of equations for the kernels of the SH, SV and P modes are obtained. For convenience, z and z' are exchanged and $\boldsymbol{P}^-(z',z',t)$ is denoted $\boldsymbol{R}(z,t)$ from now on. The system of equations for the kernel $P^+_\mathrm{sh}(z',z,t)$ of the SH mode reads

$$\begin{aligned}
\partial_z P^+_\mathrm{sh}(z',z,t) = &-a_\mathrm{sh}(z',z)\alpha_\mathrm{sh}(z,t) - \alpha_\mathrm{sh}(z)P^+_\mathrm{sh}(z',z,t) - a_\mathrm{sh}(z',z)\beta_\mathrm{sh}(z)R_\mathrm{sh}(z,t) \\
&- \left[\alpha_\mathrm{sh}(z,\cdot) * P^+_\mathrm{sh}(z',z,\cdot)\right](t) - a_\mathrm{sh}(z',z)\left[\beta_\mathrm{sh}(z,\cdot) * R_\mathrm{sh}(z,\cdot)\right](t) \\
&- \beta_\mathrm{sh}(z)\left[P^+_\mathrm{sh}(z',z,\cdot) * R_\mathrm{sh}(z,\cdot)\right](t) \\
&- \left[\beta_\mathrm{sh}(z,\cdot) * P^+_\mathrm{sh}(z',z,\cdot) * R_\mathrm{sh}(z,\cdot)\right](t).
\end{aligned}$$

The system of equations and the initial value for $R_\mathrm{sh}(z,t)$ read

$$\begin{aligned}
&\partial_z R_\mathrm{sh}(z,t) - 2s_\mathrm{t}(z)\partial_t R_\mathrm{sh}(z,t) = -2\alpha_\mathrm{sh}(z)R_\mathrm{sh}(z,t) - 2\left[\alpha_\mathrm{sh}(z,\cdot) * R_\mathrm{sh}(z,\cdot)\right](t) \\
&-\beta_\mathrm{sh}(z)\left[R_\mathrm{sh}(z,\cdot) * R_\mathrm{sh}(z,\cdot)\right](t) - \left[\beta_\mathrm{sh}(z,\cdot) * R_\mathrm{sh}(z,\cdot) * R_\mathrm{sh}(z,\cdot)\right](t) + \gamma_\mathrm{sh}(z,t).
\end{aligned}$$

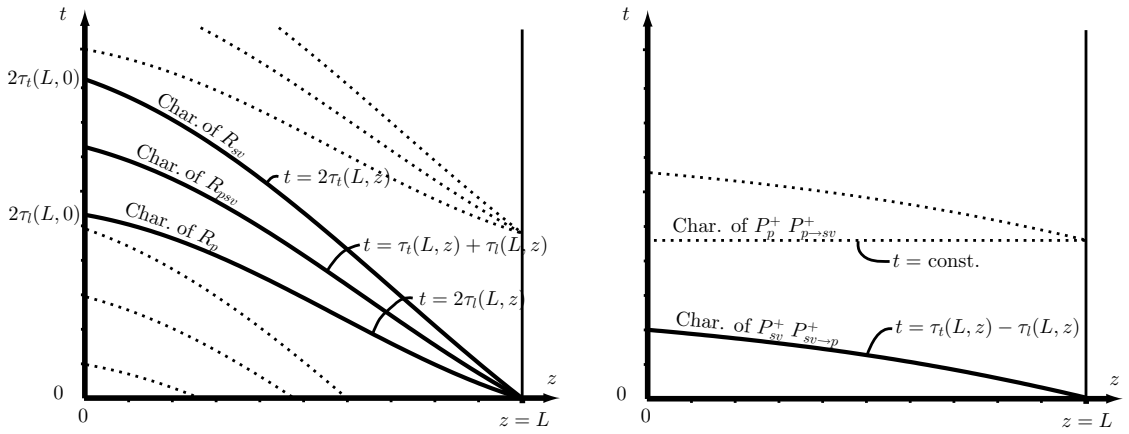

Figure 3: Some characteristic lines of the propagator kernels $\boldsymbol{R}_{\rm psv}(z,t)$ and $\boldsymbol{P}^+_{\rm psv}(L,z,t)$, i.e. the imbedding equations for a slab $0 \le z \le L$.

$$R_{\rm sh}(z,0) = -\frac{1}{2}\frac{1}{s_{\rm t}(z)}\gamma_{\rm sh}(z).$$

Note that the kernel $P^+_{\rm sh}(z',z,t)$ does not appear in this equation. The coupled system of equations for the propagator kernels $\boldsymbol{P}^+_{\rm psv}(z',z,t)$ of the SV and P modes reads

$$\begin{aligned}
&\partial_z \begin{pmatrix} P^+_{\rm sv} & P^+_{\rm p\to sv} \\ P^+_{\rm sv\to p} & P^+_{\rm p} \end{pmatrix} - \begin{pmatrix} (s_{\rm t}-s_{\rm l})\,\partial_t P^+_{\rm sv} & 0 \\ (s_{\rm t}-s_{\rm l})\,\partial_t P^+_{\rm sv\to p} & 0 \end{pmatrix} \\
&\quad = -\begin{pmatrix} a_{\rm sv}(z',z)\mathcal{S}(z',z) & 0 \\ 0 & a_{\rm p}(z',z) \end{pmatrix} \left(\boldsymbol{\alpha}_{\rm psv} + \boldsymbol{\beta}_{\rm psv}\boldsymbol{R}_{\rm psv} + \left[\boldsymbol{\beta}_{\rm psv} * \boldsymbol{R}_{\rm psv}\right]\right) \\
&\quad -\boldsymbol{P}^+_{\rm psv}\boldsymbol{\alpha}_{\rm psv} - \left[\boldsymbol{P}^+_{\rm psv} * \left(\boldsymbol{\alpha}_{\rm psv} + \boldsymbol{\beta}_{\rm psv}\boldsymbol{R}_{\rm psv} + \boldsymbol{\beta}_{\rm psv} * \boldsymbol{R}_{\rm psv}\right)\right].
\end{aligned} \tag{6.12}$$

The initial values and the jump discontinuities for the $\boldsymbol{P}^+_{\rm psv}$ kernels read

$$\begin{cases}
P^+_{\rm sv\to p}(z',z,0) & = \dfrac{a_{\rm p}(z',z)}{s_{\rm t}(z)-s_{\rm l}(z)}\alpha_{\rm psv}(z) \\
\left[P^+_{\rm p\to sv}(z',z,t)\right]_{t=\tau_{\rm t}(z,0)-\tau_{\rm l}(z,0)} & = \dfrac{a_{\rm sv}(z',z)}{s_{\rm t}(z)-s_{\rm l}(z)}\alpha_{\rm psv}(z) \\
P^+_{\rm sv}(z',z,0) & = 0.
\end{cases} \tag{6.13}$$

The coupled system of equations for the kernels $\boldsymbol{R}_{\rm psv}(z,t)$ reads

$$\begin{aligned}
&\partial_z \begin{pmatrix} R_{\rm sv} & R_{\rm p\to sv} \\ R_{\rm sv\to p} & R_{\rm p} \end{pmatrix} - \begin{pmatrix} 2s_{\rm t}\partial_t R_{\rm sv} & (s_{\rm t}+s_{\rm l})\,\partial_t R_{\rm p\to sv} \\ (s_{\rm t}+s_{\rm l})\,\partial_t R_{\rm sv\to p} & 2s_{\rm l}\partial_t R_{\rm p} \end{pmatrix} \\
&\quad = \boldsymbol{\gamma}_{\rm psv} - \boldsymbol{\alpha}_{\rm psv}\boldsymbol{R}_{\rm psv} - \left[\boldsymbol{\alpha}_{\rm psv} * \boldsymbol{R}_{\rm psv}\right] - \boldsymbol{R}_{\rm psv}\boldsymbol{\alpha}_{\rm psv} - \left[\boldsymbol{R}_{\rm psv} * \boldsymbol{\alpha}_{\rm psv}\right] \\
&\quad - \left[\boldsymbol{R}_{\rm psv} * \boldsymbol{\beta}_{\rm psv}\boldsymbol{R}_{\rm psv}\right] - \left[\boldsymbol{R}_{\rm psv} * \boldsymbol{\beta}_{\rm psv} * \boldsymbol{R}_{\rm psv}\right],
\end{aligned} \tag{6.14}$$

where $R_{\rm p\to sv}(z,t) = -R_{\rm sv\to p}(z,t)$, i.e. there are only three independent systems of equations in Eq. (6.14) since the system of equations for $R_{\rm p\to sv}(z,t)$ and $-R_{\rm sv\to p}(z,t)$

are identical. The initial values of the kernels $\boldsymbol{R}_{\rm psv}(z,t)$ read

$$\begin{cases} R_{\rm sv}(z,0) & = -\dfrac{1}{2}\dfrac{1}{s_{\rm t}(z)}\gamma_{\rm sv}(z) \\ R_{\rm p\to sv}(z,0) & = \dfrac{1}{s_{\rm t}(z)+s_{\rm l}(z)}\beta_{\rm psv}(z) \\ R_{\rm p}(z,0) & = -\dfrac{1}{2}\dfrac{1}{s_{\rm l}(z)}\gamma_{\rm p}(z). \end{cases} \tag{6.15}$$

Note that the system of equations for the kernel $\boldsymbol{R}_{\rm psv}(z,t)$ in Eq. (6.14) does not depend upon the kernel $\boldsymbol{P}^{+}_{\rm psv}(z',z,t)$. This is an attractive feature in the inverse problem, where the reflection kernels are the input data, since only the system in Eq. (6.14) is solved independently of the system in Eq. (6.12). In the Green functions approach, the kernels $\boldsymbol{P}^{-}_{\rm psv}(z',z,t)$ are coupled to the kernels $\boldsymbol{P}^{+}_{\rm psv}(z',z,t)$ and these kernels have to be solved simultaneously and several discontinuities have to be taken care of. However, the imbedding equations are more time consuming to solve since they include double convolutions. From the left hand side of eqs. (6.12) and (6.14), the characteristics of the kernels $\boldsymbol{R}_{\rm psv}(z,t)$ and $\boldsymbol{P}^{+}_{\rm psv}(L,z,t)$ are obtained, see Section 7.2. Some of the corresponding characteristic lines for a slab $0 \le z \le L$ are presented in Figure 3. The attenuation factors are given in Eq. (6.9).

7 The direct and the inverse problem

In this section, a numerical algorithm for the inverse P-SV problem based upon the imbedding equations is presented. The numerical algorithm for the uncoupled SH mode is simpler and will not be described here. The imbedding equations are chosen since they are simpler to treat numerically than the Green kernel equations. In the imbedding method, three kernels are to be determined, namely $R_{\rm sv}(z,t)$, $R_{\rm psv}(z,t)$ and $R_{\rm p}(z,t)$, involving three different characteristics. In the Green functions approach, eight coupled kernels are to be determined involving four different characteristics. Furthermore, the Green kernels $G^{-}_{\rm p\to sv}(z,t)$ and $G^{-}_{\rm sv\to p}(z,t)$ are only equal at $z=0$, except for the sign, and inside the slab two different systems of equations are to be solved for the kernels $G^{-}_{\rm p\to sv}(z,t)$ and $G^{-}_{\rm sv\to p}(z,t)$.

The input data to the inverse problem are the synthetic reflection kernels obtained by by solving the direct problem. The direct problem is solved by the Green functions approach in order to get a different system of equations than the imbedding system used in the inverse problem. The numerical algorithm for the Green kernel equations for the direct problem used in the numerical examples, is based upon the same ideas as the numerical algorithm for the imbedding equations.

7.1 The direct problem

The direct problem is to determine the reflection kernel $\boldsymbol{R}(t)$ and, if wanted, the transmission kernel $\boldsymbol{T}(t)$ in Eq. (4.7). Examples of the numerical algorithm for simpler cases can be found in e.g. [17] for the Green functions approach and in [25] for the compact Green functions approach.

In the Green functions approach, Eq. (6.4) is to be solved together with the initial values in eqs. (6.5) and (6.6) and the boundary values in Eq. (5.2). The jump discontinuities are given by Eq. (6.7). Since the kernels are coupled to each other, the kernels and the system of equations have to be solved simultaneously. In the Green function approach, the initial values at a point $z = z'$ are propagated by the equations of the kernels $\boldsymbol{G}^-$ along the characteristic lines $t = 2\tau_{\rm l}(z, z')$ and $t = \tau_{\rm t}(z, z') - \tau_{\rm l}(z, z')$, up to the reflection kernels $\boldsymbol{G}(z = 0, t) = \boldsymbol{R}(t)$ at $z = 0$, see Figure 2. The kernels $\boldsymbol{G}^+$ are propagated from $z = 0$ along the characteristic lines $t = const.$ and $t = \tau_{\rm t}(z, z') - \tau_{\rm l}(z, z')$, to $z = L$ giving the transmission kernels $\boldsymbol{G}(z = L, t) = \boldsymbol{T}(t)$.

The direct problem for the imbedding method is to solve Eq. (6.14) together with the initial values in Eq. (6.15) and the boundary values in Eq. (5.5). The initial values at a point z' are propagated by the equations of the kernels $R_{\rm sv}, R_{\rm psv}$ and $R_{\rm p}$ along the characteristic lines $t = 2\tau_{\rm t}(z, z')$, $t = \tau_{\rm t}(z, z') + \tau_{\rm l}(z, z')$ and $t = 2\tau_{\rm l}(z, z')$, respectively, up to the reflection kernels, see Figure 3. The transmission kernel can then be determined using eqs. (5.5), (6.12) and (6.13).

7.2 The inverse problem

In this subsection, a numerical algorithm for the P-SV imbedding equations is presented. The inverse problem is to determine the material parameters of the slab from the reflection kernel $\boldsymbol{R}(t)$. In the P-SV case, there are three reflection kernels given, $R_{\rm sv}(t)$, $R_{\rm psv}(t)$ and $R_{\rm p}(t)$, indicating that three parameters of the slab can be determined from the three kernels for one given value of the parameter α in Eq. (3.1). The three parameters are the density $\rho(z)$ and the spatial dependence of the shear and elasticity modulus, $G(z, t)$ and $E(z, t)$, where the time dependence is assumed to be known. In the numerical section, it is also assumed that the spatial and time dependence of the modulus $G(z, t)$ and $E(z, t)$ can be separated into two functions

$$\begin{aligned} G(z, t) &= G(z)g(t) \\ E(z, t) &= E(z)e(t). \end{aligned} \tag{7.1}$$

These separations make the functions $h(z, t)$ and $f(z, t)$ independent of z, cf. Eq. (3.6), but they are not applicable for all classes of viscoelastic media, see e.g. [1].

The imbedding equations are solved by means of the method of characteristics. The equations are integrated along their characteristic lines by the trapezoidal rule. The characteristic lines of the imbedding kernels are, cf. Eq. (6.14) and Figure 3

$$\begin{aligned} R_{\rm sv}(z, t): &\quad t = 2\tau_{\rm t}(z, z') \\ R_{\rm psv}(z, t): &\quad t = \tau_{\rm t}(z, z') + \tau_{\rm l}(z, z') \\ R_{\rm p}(z, t): &\quad t = 2\tau_{\rm l}(z, z'), \end{aligned} \tag{7.2}$$

where z' is the point where the characteristic line intercepts the z-axis. The discretization is chosen to be uniform both in z and t, and Δt and Δz are defined in

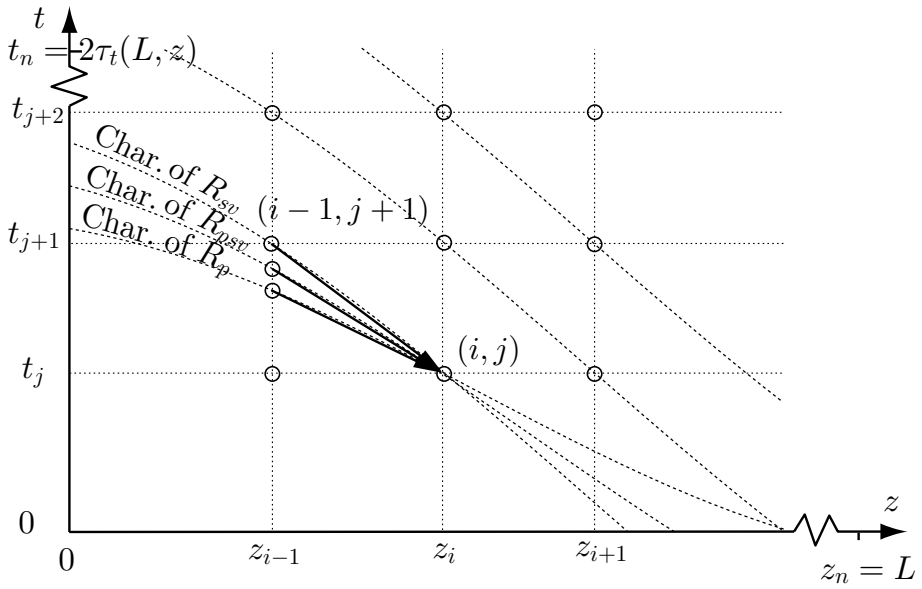

Figure 4: The grid for the computation of the kernels $R_{\rm sv}$, $R_{\rm psv}$ and $R_{\rm p}$ in the point (z_i, t_j).

the SV system as

$$\begin{aligned} &\Delta t = t_j - t_{j-1} = \frac{2\tau_{\rm t}(0,L)}{n}, \\ &\Delta z(i) = \{\Delta t = 2\tau_{\rm t}(z(i-1), z(i))\} = z(i) - z(i-1), \end{aligned} \tag{7.3}$$

where n is the number of gridpoints. Interpolation in time is needed for the kernels $R_{\rm psv}(z,t)$ and $R_{\rm p}(z,t)$ since their characteristics do not intercept the chosen discretization grid, see Figure 4. In the remaining of this section, the discretization gridpoints $(z(i), t_j)$ are denoted (i,j) or z_i, t_j. The derivatives in terms of z and t along the characteristics of $\boldsymbol{R}_{\rm psv}$ in Eq. (6.14) are rewritten in terms of z only using the characteristic Eq. (7.2)

$$\begin{array}{lll} \partial_z R_{\rm sv} - 2s_{\rm t}\partial_t R_{\rm sv} & = \partial_z R_{\rm sv} + \frac{dt}{dz}\partial_t R_{\rm sv} & = d_z R_{\rm sv}(z,t) \\ \partial_z R_{psv} - (s_{\rm l} + s_{\rm t})\,\partial_t R_{psv} & = \partial_z R_{psv} + \frac{dt}{dz}\partial_t R_{psv} & = d_z R_{psv}(z,t) \\ \partial_z R_{\rm p} - 2s_{\rm t}\partial_t R_{\rm p} & = \partial_z R_{\rm p} + \frac{dt}{dz}\partial_t R_{\rm p} & = d_z R_{\rm p}(z,t) \end{array}$$

Then the trapezoidal rule is applied to Eq. (6.14) that is integrated along its characteristic. As an example, the equation for $R_{\rm sv}$ is integrated from $(i-1, j+1)$ down to (i,j), see Figure 4

$$R_{\rm sv}(i,j) - R_{\rm sv}(i-1,j) = \frac{z(i) - z(i-1)}{2}\left(RHS_{\rm sv}(i,j) + RHS_{\rm sv}(i-1,j+1)\right), \tag{7.4}$$

where $RHS_{\rm sv}(i,j)$ denotes the right hand side of the $R_{\rm sv}$ equation in Eq. (6.14). $RHS_{\rm sv}(i,j)$ is a function of the kernels $R_{\rm sv}$, $R_{\rm psv}$ and $R_{\rm p}$ and the parameters of the medium, see [17] for details. The trapezoidal rule is also used for the integration of the $R_{\rm psv}$ and $R_{\rm p}$ equations along their characteristics giving similar equations as Eq. (7.4). In this case, the points at z_{i-1} do not intercept the point $(i-1, j+1)$ and an interpolation or extrapolation in time is needed. This interpolation causes problems, since the information will not strictly propagate along a single characteristic. The interpolation in the present problem is linear close to the characteristics and of simple quadratic type elsewhere. Much effort has been paid on the interpolation problem. However, the results have not been too successful, see the reconstructed profiles in Figure 5, but it is plausible that an algorithm can be improved on this point.

The three equations similar to Eq. (7.4) are solved simultaneously in order to determine $R_{\rm sv}(i,j)$, $R_{\rm psv}(i,j)$ and $R_{\rm p}(i,j)$. The gridpoints for the computation of the kernels $\boldsymbol{R}^{\pm}_{\rm psv}$ at a point (i,j) are presented in Figure 4.

7.3 The inverse scheme

The inverse scheme is summarized as follows

Step 0: Initialize. Set i=0. The boundary values in Eq. (5.5) are used to initialize the grid at $z(i=0)=0$. The time step $\Delta t = 2\tau_{\rm t}(0,L)/n$ is unknown since $2\tau_{\rm t}(0,L)$ depends upon the so far unknown parameters $\rho(z)$ and $G(z)$. In this case, Δt is approximated so that $z(n) \approx L$. The kernels $R_{\rm sv}(0,j)$,$R_{\rm psv}(0,j)$ and $R_{\rm p}(0,j)$ are then initialized using the reflection kernels from the direct problem.

Step 1: Determine the parameters at the point z_i. Set i:=i+1. The three parameters $\rho(z_i)$, $G(z_i)$ and $E(z_i)$ with given time dependence are to be determined at z_i. The kernels $R_{\rm sv}(i,j=0)$, $R_{\rm psv}(i,j=0)$ and $R_{\rm p}(i,j=0)$ are determined from Eq. (7.4) and related equations for $R_{\rm psv}$ and $R_{\rm p}$. The initial value in Eq. (6.15) is used to determine the parameters at the point z_i in the following way

$$\begin{pmatrix} \frac{\rho_z(i)}{\rho(i)} \\ \frac{G_z(i)}{G(i)g(0)} \\ \frac{E_z(i)}{E(i)e(0)} \end{pmatrix} = \begin{pmatrix} \frac{1}{4}\frac{1-2\alpha^2 c_{\rm t}(i)^2}{1-\alpha^2 c_{\rm t}(i)^2} & \frac{1}{4}\frac{1}{1-\alpha^2 c_{\rm t}(z)^2} - 2\alpha^2\frac{G(i)g(0)}{\rho(i)} & 0 \\ \frac{1}{2}\frac{\alpha}{s(i)} & -\frac{1}{2}\frac{\alpha G(i)g(0)}{\rho(i)}\left(s(i) - \frac{\alpha^2}{s(i)}\right) & 0 \\ \frac{1}{4}\frac{1-2\alpha^2 c_{\rm l}(i)^2}{1-\alpha^2 c_{\rm l}(i)^2} & -2\alpha^2\frac{G(i)g(0)}{\rho(i)} & \frac{1}{4}\frac{1}{1-\alpha^2 c_{\rm l}(i)^2} \end{pmatrix} \begin{pmatrix} -2s_{\rm t}(i)R_{\rm sv}(z,0) - \frac{1}{2}Z_{\rm sv}(i)\frac{h(0)}{g(0)} \\ -2\frac{s_{\rm t}(i)+s_{\rm l}(i)}{s_{\rm t}(i)s_{\rm l}(i)}R_{\rm psv}(z,0) \\ -2s_{\rm l}(i)R_{\rm p}(z,0) - \frac{1}{2}Z_{\rm p}(i)\frac{f(0)}{e(0)} \end{pmatrix}$$

where $s(i) = \sqrt{s_{\rm l}(i)s_{\rm t}(i)}$. Note that an iteration process has to be used since the parameters that are to be determined at z_i are needed to determine the discretization step z_i in Eq. (7.3). The parameters are also needed for the

determination of the points on the time-axis where the numerical integration of $R_{\rm psv}$ and $R_{\rm p}$ starts, see Figure 4.

Step 2: Determine the kernels *R*. The three equations similar to Eq. (7.4) for the three kernels are used to determine the kernels $R_{\rm sv}(i,j)$,$R_{\rm psv}(i,j)$ and $R_{\rm p}(i,j)$ from $j=1$ up to $j=n-i$.

Step 3: Repeat. Repeat step 1 until $z_i \geq L$, where L is the length of the slab.

8 Numerical examples

In this section, one numerical example for the P-SV case is presented. The number of discretization steps n is chosen to $n=200$ in the direct problem and $n=150$ in the inverse problem and the length of the slab is $L=1$ m. The important issue concerning the influence of noisy data is not considered in this paper. The chosen profiles of the density $\rho(z)$ and the spatial dependence of the shear and elasticity modulus $G(z)$ and $E(z)$ are presented in Figure 5. The reconstruction of the time dependence of the shear and elasticity modulus, $g(t)$ and $e(t)$, is not considered here. The reconstruction of the function $g(t)$ for a homogeneous viscoelastic medium has already been treated for the SH case in [2] using reflection data and in [19] using transmission data. The time dependence of the shear and the elasticity modulus, the parameters $g(t)$ and $e(t)$ in Eq. (7.1), are prescribed and given by the Maxwell(Debye) model, cf. [1]

$$g(t) = g(0)\exp\left(-\frac{t}{\tau_g}\right), \qquad e(t) = e(0)\exp\left(-\frac{t}{\tau_e}\right), \tag{8.1}$$

where $g(0)=e(0)=1$, $\tau_g=1$ for the shear modulus and $\tau_e=10$ for the elasticity modulus. Note that the resolvent kernels are constant, $h(t)=const.=-1/\tau_g$ and $f(t)=const.=-1/\tau_e$, for the Maxwell(Debye) model, cf. Eq. (3.6). The parameter α in Eq. (3.1) is chosen to $\alpha=0.2$. In the first numerical example, the reflection kernels $R_{\rm sv}(z,t)$, $R_{\rm psv}(z,t)$ and $R_{\rm p}(z,t)$ are determined from the Green functions equations described in Section 7.1. The inverse problem using the reflection kernels $R_{\rm sv}(z,t)$, $R_{\rm psv}(z,t)$ and $R_{\rm p}(z,t)$ as input data is then solved by the imbedding method described in Section 7.2. The reconstructed profiles of $\rho(z)$, $G(z)$ and $E(z)$ are the dashed lines presented in Figure 5. As seen from this figure, the reconstruction deviates more and more for larger z. A reason for this is that the interpolation in time in the numerical algorithm causes the information deviate from the characteristics.

A less successful attempt was done to determine the three parameters $\rho(z)$, $G(z)$ and $E(z)$ in an inverse problems with three simpler equations than in the previous example. These three equations were the two uncoupled P-SV equations ($\alpha=0$) together with a SH equation for the oblique case ($\alpha\neq 0$). The numerical solutions did never converge all the way through the slab indicating that this problem is ill-conditioned and hence very sensitive to noise. A plausible explanation is that the difference between the SV and the SH kernels is too small. This problem did not

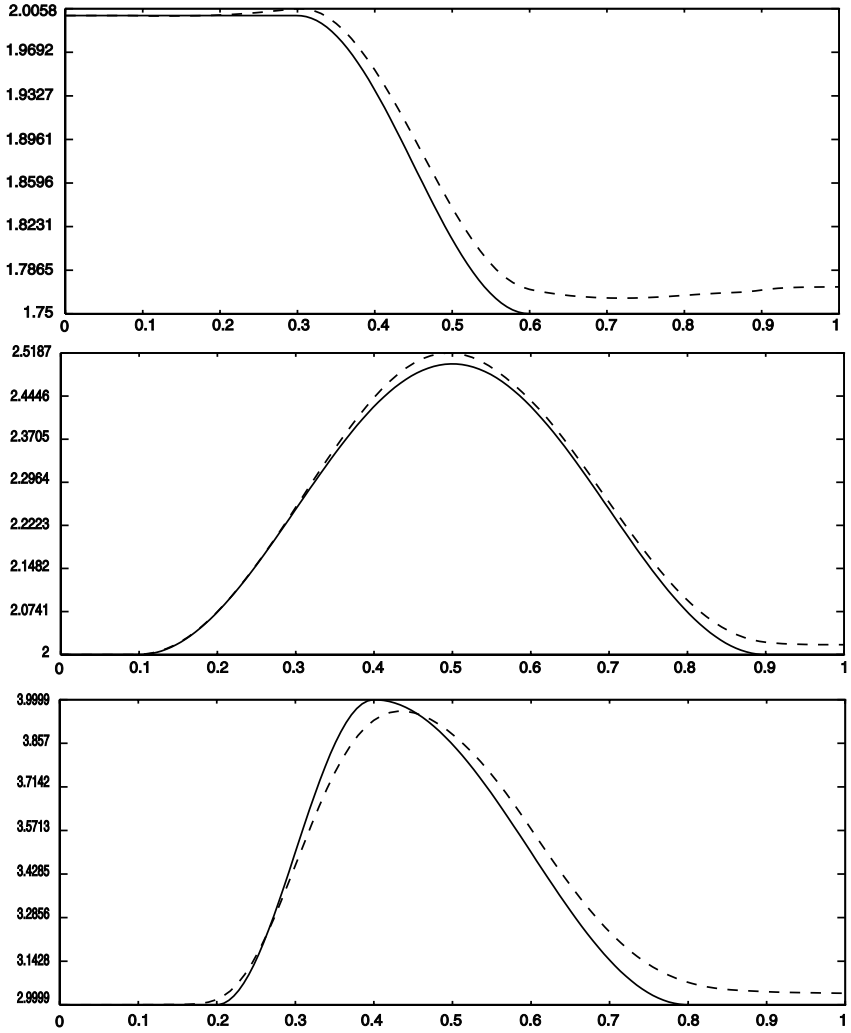

Figure 5: The solid lines are the chosen profiles of the density $\rho(z)$ and the spatial dependence of the shear and elasticity modulus $G(z)$ and $E(z)$. The dashed lines are the corresponding reconstructed profiles.

occur for the coupled P-SV case in the previous example. In [28], it is shown that the reflectivity functions do not change very much over a large band of angles which may be the problem also in the present case.

Finally, it is remarked that the inverse problem of reconstructing three parameters is a delicate problem. The reconstruction of one parameter is much easier, and for this case, an almost exact reconstruction can be obtained.

9 Conclusions

The wave propagator concept is applied to a viscoelastic medium excited by obliquely incident transient plane waves of SH and P-SV type. Two different systems of equations for the corresponding propagator kernels, both for the SH mode and the cou-

pled P-SV modes, are derived. One system of equations is closely related to the Green kernel equations and the other to the imbedding kernel equations. The relations between the wave propagators, the imbedding method and the Green functions technique are also discussed. For the P-SV case, it turns out that the imbedding equations are easier to treat numerically than the Green functions equations. However, the Green functions approach gives a better physical understanding of the scattering problem since the Green kernels correspond to forward and backward scattering at each point inside the medium. The direct and the inverse scattering for a slab is also discussed where a numerical example for the P-SV case is presented.

There are several possible application of the presented method. An interesting application is the design of non-reflecting viscoelastic media where the inverse problem is to be solved given that the reflection kernel is identically zero, cf. [17].

Acknowledgment

The presented work has been supported by the Swedish Research Council for Engineering Sciences that is gratefully acknowledged.

Appendix A The elements in the $\mathcal{C}$ matrix

In this appendix the elements in the matrix valued operator $\mathcal{C}$ in eq. (3.11) are presented. The functions for the SH mode in the $\mathcal{C}$ matrix mode read

$$\begin{cases} \alpha_{sh} = \dfrac{1}{2}\rho\dfrac{h(z,0)}{Z_{sh}} \\ \beta_{sh} = \dfrac{1}{2}\partial_z \ln Z_{sh}(z) - \dfrac{1}{2}\rho\dfrac{h(z,0)}{Z_{sh}}\left(1 - 2\alpha^2\dfrac{G(z,0)}{\rho}\right) \\ \gamma_{sh} = \dfrac{1}{2}\partial_z \ln Z_{sh}(z) + \dfrac{1}{2}\rho\dfrac{h(z,0)}{Z_{sh}}\left(1 - 2\alpha^2\dfrac{G(z,0)}{\rho}\right) \\ \tilde{\alpha}_{sh} = \dfrac{1}{2}\left(\dfrac{\alpha^2}{Z_{sh}}G_{tt} + \dfrac{Z_{sh}}{G(z,0)}h_t\right) \\ \tilde{\beta}_{sh} = -\tilde{\gamma}_{sh} = \dfrac{1}{2}\left(\dfrac{\alpha^2}{Z_{sh}}G_{tt} - \dfrac{Z_{sh}}{G(z,0)}h_t\right). \end{cases}$$

The functions for the SV mode in the $\boldsymbol{\mathcal{C}}$ matrix read

$$\begin{cases} \alpha_{sv} = \dfrac{1}{2} Z_{sv} \dfrac{h(z,0)}{G(z,0)} \\ \beta_{sv} = \dfrac{1}{2} \partial_z \ln Z_{sv}(z) - \dfrac{1}{2} \left(Z_{sv} \dfrac{h(z,0)}{G(z,0)} + 4 \dfrac{\alpha^2}{\rho} G_z(z,0) \right) \\ \gamma_{sv} = \dfrac{1}{2} \partial_z \ln Z_{sv}(z) + \dfrac{1}{2} \left(Z_{sv} \dfrac{h(z,0)}{G(z,0)} - 4 \dfrac{\alpha^2}{\rho} G_z(z,0) \right) \\ \tilde{\alpha}_{sv} = \dfrac{1}{2} \dfrac{Z_{sv}}{G(z,0)} h_t \\ \tilde{\beta}_{sv} = -\dfrac{1}{2} \left(\dfrac{Z_{sv}}{G(z,0)} h_t + 4 \dfrac{\alpha^2}{\rho} G_{zt} \right) \\ \tilde{\gamma}_{sv} = \dfrac{1}{2} \left(\dfrac{Z_{sv}}{G(z,0)} h_t - 4 \dfrac{\alpha^2}{\rho} G_{zt} \right). \end{cases}$$

The functions for the P mode in the $\boldsymbol{\mathcal{C}}$ matrix read

$$\begin{cases} \alpha_{p} = \dfrac{1}{2} Z_{p} \dfrac{f(z,0)}{E(z,0)} \\ \beta_{p} = \dfrac{1}{2} \partial_z \ln Z_{p}(z) - \dfrac{1}{2} \left(Z_{p} \dfrac{f(z,0)}{E(z,0)} + 4 \dfrac{\alpha^2}{\rho} G_z(z,0) \right) \\ \gamma_{p} = \dfrac{1}{2} \partial_z \ln Z_{p}(z) + \dfrac{1}{2} \left(Z_{p} \dfrac{f(z,0)}{E(z,0)} - 4 \dfrac{\alpha^2}{\rho} G_z(z,0) \right) \\ \tilde{\alpha}_{p} = \dfrac{1}{2} \dfrac{Z_{p}}{E(z,0)} f_t \\ \tilde{\beta}_{p} = -\dfrac{1}{2} \left(\dfrac{Z_{p}}{E(z,0)} f_t + 4 \dfrac{\alpha^2}{\rho} G_{zt} \right) \\ \tilde{\gamma}_{p} = \dfrac{1}{2} \left(\dfrac{Z_{p}}{E(z,0)} f_t - 4 \dfrac{\alpha^2}{\rho} G_{zt} \right). \end{cases}$$

Finally, the functions α_{psv}, β_{psv}, $\tilde{\alpha}_{psv}$ and $\tilde{\beta}_{psv}$ in the matrix $\boldsymbol{\mathcal{C}}$ read

$$\begin{cases} \alpha_{psv} = -\dfrac{\alpha}{\rho \sqrt{s_t s_l}} \left(\dfrac{1}{2} \partial_z \rho(z) + \left(s_t s_l + \alpha^2 \right) G_z(z,0) \right) \\ \beta_{psv} = \dfrac{\alpha}{\rho \sqrt{s_t s_l}} \left(\dfrac{1}{2} \partial_z \rho(z) - \left(s_t s_l - \alpha^2 \right) G_z(z,0) \right) \\ \tilde{\alpha}_{psv} = -\dfrac{\alpha}{\rho \sqrt{s_t s_l}} \left(s_t s_l + \alpha^2 \right) G_{zt} \\ \tilde{\beta}_{psv} = -\dfrac{\alpha}{\rho \sqrt{s_t s_l}} \left(s_t s_l - \alpha^2 \right) G_{zt}. \end{cases}$$

References

[1] J. J. Aklonis and J. W. MacKnight. *Introduction to Polymer Viscoelasticity.* John Wiley and Sons, 1983.

[2] E. Ammicht, J.P. Corones, and R.J. Krueger. Direct and inverse scattering for viscoelastic media. *J. Acoust. Soc. Am.*, **81**, 827–834, 1987.

[3] D.V.J. Billger and P.D. Folkow. The reflection equation for the Timoshenko beam. Technical Report 2, Division of Mechanics, Chalmers University of Technology, 1996.

[4] D.V.J. Billger and P.D. Folkow. The transmission equation for the Timoshenko beam. Technical Report 3, Division of Mechanics, Chalmers University of Technology, 1996.

[5] K. Bube and R. J. Burrridge. The one-dimensional inverse problem of reflection seismology. *SIAM Review*, **25**(4), 497–559, 1983.

[6] J. Carazzone. Inversion of p-sv seismic data. *Geophysics*, **51**(5), 1056–1068, 1986.

[7] T. J. Clarke. Full reconstruction of a layered elastic medium from p-sv slant-stack data. *Geophys. J. R. astr. Soc.*, **78**, 775–793, 1984.

[8] J.P. Corones, M.E. Davison, and R.J. Krueger. Direct and inverse scattering in the time domain via invariant imbedding equations. *J. Acoust. Soc. Am.*, **74**(5), 1535–1541, 1983.

[9] J.P. Corones and A. Karlsson. Transient direct and inverse scattering for inhomogeneous viscoelastic media: obliquely incident SH mode. *Inverse Problems*, **4**, 643–660, 1988.

[10] Achenbach J. D. *Wave propagation in elastic solids*. North-Holland, 1984.

[11] R.P. Dougherty. *Direct and inverse scattering of classical waves at oblique incidence to stratified media via invariant imbedding equations*. PhD thesis, Iowa State University, Ames, Iowa, 1986.

[12] P.D. Folkow, G. Kristensson, and Peter Olsson. Time domain Green functions for the homogeneous Timoshenko beam. *QJMAM*, 1997. (accepted for publication).

[13] J. Fridén, G. Kristensson, and R.D. Stewart. Transient electromagnetic wave propagation in anisotropic dispersive media. *J. Opt. Soc. Am. A*, **10**(12), 2618–2627, 1993.

[14] R. Hall and P. Sacks. Impedance inversion from transmission data for the wave equation. *Wave Motion*, **24**, 263–274, 1996.

[15] S. He. A 'compact Green function' approach to the time domain direct and inverse problems for a stratified dissipative slab. *J. Math. Phys.*, **34**(10), 4628–4645, 1993.

[16] S. He. Frequency and time domain Green functions technique for nonuniform LCRG transmission lines with frequency-dependent parameters. *J. Electro. Waves Applic.*, **7**(1), 31–48, 1993.

[17] R. Hellberg. Design of reflectionless slabs for obliquely incident transient electromagnetic waves. *Inverse Problems*, **13**, 97–112, 1997.

[18] R. Hellberg and A. Karlsson. Design of reflectionless media for transient electromagnetic waves. *Inverse Problems*, **11**, 147–164, 1995.

[19] A. Karlsson. Inverse scattering for viscoelastic media using transmission data. *Inverse Problems*, **3**, 691–709, 1987.

[20] A. Karlsson. Wave propagators for transient waves in one-dimensional media. *Wave Motion*, **24**(1), 85–99, 1996.

[21] A. Karlsson, H. Otterheim, and R. Stewart. Electromagnetic fields in an inhomogeneous plasma from obliquely incident transient plane waves. *Radio Science*, **28**(3), 365–378, 1993.

[22] B. L. N. Kenneth. Seismic waves in laterally inhomogeneous media. *Geophys. J. R. astr. Soc.*, **27**, 301–325, 1972.

[23] G. Kristensson. Direct and inverse scattering problems in dispersive media—Green's functions and invariant imbedding techniques. In R. Kleinman, R. Kress, and E. Martensen, editors, *Direct and Inverse Boundary Value Problems*, Methoden und Verfahren der Mathematischen Physik, Band 37, pages 105–119, Frankfurt am Main, 1991. Peter Lang.

[24] R.J. Krueger and R.L. Ochs, Jr. A Green's function approach to the determination of internal fields. *Wave Motion*, **11**, 525–543, 1989.

[25] J. Lundstedt and S. He. Signal restoration after transmission through a nonuniform *LCRG* line. *IEEE Trans. Microwave Theory Tech.*, **42**(11), 2087–2092, 1994.

[26] J. Lundstedt and S. Ström. Simultaneous reconstruction of two parameters from the transient response of a nonuniform LCRG transmission line. *J. Electro. Waves Applic.*, **10**(1), 19–50, 1996.

[27] P. Olsson and G. Kristensson. Wave splitting of the Timoshenko beam equation in the time domain. *Zeitschrift für andgewandte Mathematik und Physik*, **45**, 866–881, 1994.

[28] P. E. Sacks and W. W. 1990 Symes. The inverse problem for a fluid over a layered elastic half-space. *Wave Motion*, **6**, 1031–1054, 1990.

[29] D. C. Stickler. Inverse scattering for stratified elastic media. *Wave Motion*, **8**, 101–112, 1986.

[30] V.H. Weston. Invariant imbedding and wave splitting in $\mathbb{R}^3$: II. The Green function approach to inverse scattering. *Inverse Problems*, **8**, 919–947, 1992.